5 ng/ml of each cytokine was the optimal concentration for stimulating RASFs.

**Cell proliferation assay.** Cell growth was assessed by incorporation of $^3$H-thymidine. Three days after the adenoviral infection, RASFs were stimulated for 36 hours with IL-1$\beta$, TNF$\alpha$, or indomethacin. $^3$H-thymidine (0.3 $\mu$Ci; Amersham Biosciences, Buckinghamshire, UK) was added during the last 24 hours of culture, and the incorporated radioactivities were quantified. Numbers of live cells were determined using Cell Counting Kit 8 (Dojin, Kumamoto, Japan).

**Flow cytometry for cell cycle analysis.** Cells were fixed in phosphate buffered saline containing 0.15% Triton X-100 for 10 minutes, and then incubated with 50 $\mu$g/ml of propidium iodide (Sigma) and 5 $\mu$g/ml of RNase A. Cells were analyzed using a FACSCalibur (BD Biosciences, San Diego, CA), and data were collected.

**Northern blot and real-time polymerase chain reaction (PCR) analyses.** Northern blot analyses to detect MMP-3, MCP-1, and IL-1RI mRNA were performed as described elsewhere (8). Real-time PCR was performed using iQ SYBR Green Supermix (Bio-Rad, Hercules, CA) and sets of primers specific for MMP-3 (22) or MCP-1 (23) complementary DNA. Data were standardized against human GAPDH mRNA using the threshold cycle method (24).

**Enzyme-linked immunosorbent assay (ELISA).** The adenovirus-infected RASFs were cultured for 60 hours and transferred to microwells. Twelve hours after transfer, the culture supernatants were replaced with fresh Dulbecco's modified Eagle's medium containing 10% fetal bovine serum with IL-1$\beta$, TNF$\alpha$, and indomethacin. Supernatants from this 24-hour culture were collected, and levels of MMP-3 (Fuji Chemical, Toyama, Japan), MCP-1 (BioSource International, Camarillo, CA), macrophage inflammatory protein 3$\alpha$ (MIP-3$\alpha$; R&D Systems, Minneapolis, MN), and IL-6 (BioSource International) were determined by ELISA.

**Analysis of the effects of a small-molecule CDK-4/6 inhibitor.** A CDK-4/6 inhibitor, CDK4I (2-bromo-12,13-dihydro-5*H*-indolo[2,3-a]pyrrolo[3,4-c]carbazole-5,7(6*H*)-dione; Merck, Whitehouse Station, NJ) (25), was dissolved in DMSO and added to the culture medium. RASFs were pretreated with CDK4I for 6 hours. The RASFs were then stimulated with IL-1$\beta$ and TNF$\alpha$ for either 36 hours (for cell and culture supernatant analysis) or 12 hours (for RNA extraction and analysis).

**Immunoprecipitation and Western blot analyses.** For immunoprecipitation, cell lysates of RASFs were prepared on day 3 after adenovirus infection (4,8). JNKs 1–3 were immunoprecipitated using mouse anti-JNK monoclonal antibody (sc-7345; Santa Cruz Biotechnology, Santa Cruz, CA) (26). Rabbit anti-human p16$^{INK4a}$, mouse anti-human p18$^{INK4c}$, and p21$^{Cip1}$ polyclonal antibodies (sc-468, sc-9965, and sc-387, respectively; Santa Cruz Biotechnology) were used as primary antibodies for Western blot analyses.

**Multiwell colorimetric transcription factor assays.** To assess transcription factors and JNK activities in RASFs, nuclear extracts were prepared using a nuclear extract kit (Active Motif, Carlsbad, CA). Trans AM AP-1/c-Jun, NF-$\kappa$Bp50, and NF-$\kappa$Bp65 transcription factor assay kits (Active Motif) were used to quantify DNA binding activities of AP-1 and NF-$\kappa$B transcription factors.

**Statistical analysis.** $^3$H-thymidine incorporation, signal intensity ratios from the real-time PCRs, and protein concentrations in the supernatants were compared by Student's paired *t*-test using StatView 5.0J software (SAS Institute, Cary, NC).

## RESULTS

**Suppression of RASF production of MMP-3 and MCP-1 production by p16$^{INK4a}$, but no down-regulation of IL-1RI expression or association with JNK.** RASFs derived from joints with active rheumatoid inflammation were cultured in vitro. It has been shown that endogenous p16$^{INK4a}$ is not expressed in cultured RASFs (4). Cells were infected with the AxCAp16 adenovirus containing the human p16$^{INK4a}$ gene or with the control Ax1w1 blank adenovirus. When the transgene expression was at the highest level, the cells were examined for proliferation and cell cycle progression.

$^3$H-labeled thymidine incorporation by the p16$^{INK4a}$-expressing RASFs was profoundly suppressed as compared with incorporation by RASFs infected with control virus. This suppression was accompanied by an increase in the number of cells in the $G_0/G_1$ phase of the cell cycle (Figure 1A).

Preliminary DNA array analyses of gene expression in RASFs samples with and without gene transfer of p16$^{INK4a}$ suggested that a set of genes related to RA pathology, including MMP-3 and MCP-1, was down-regulated by p16$^{INK4a}$. In RASFs in which the p21$^{Cip1}$ gene had been transfected, the expression of those 2 molecules as well as MIP-3$\alpha$ and IL-6 was found to be down-regulated (8). Therefore, we next tested the expression of all 4 molecules in stimulated RASFs with and without p16$^{INK4a}$ gene transfer, using a specific ELISA. When p16$^{INK4a}$ was introduced into RASFs, the production of both MMP-3 and MCP-1 in culture supernatants was suppressed, whereas the production of MIP-3$\alpha$ and IL-6 was essentially unaffected (Figure 1B). In contrast, the overexpression of p16$^{INK4a}$ in OASFs and in NHDF-Ad did not appreciably alter the production of MMP-3 and MCP-1 (Figure 1C).

Because of variations in basal and up-regulated levels of MMP-3, MCP-1, MIP-3$\alpha$, and IL-6 in culture supernatants, their production by stimulated RASFs was assessed relative to that of control RASFs infected with control adenovirus. Typically, culture supernatants from stimulated RASFs contained approximately 500, 50, 3, and 300 ng/ml of MMP-3, MCP-1, MIP-3$\alpha$, and IL-6, respectively. The relative production of MMP-3 and IL-6 protein by stimulated RASFs infected with the control Ax1w1 adenovirus as compared with uninfected

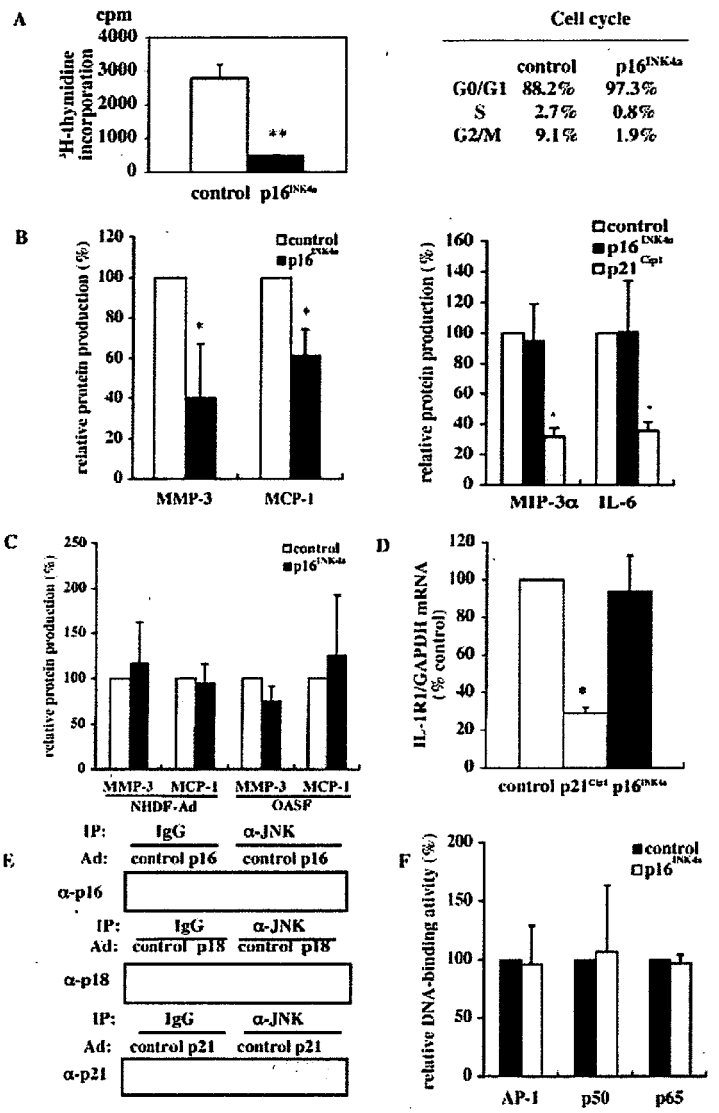


**Figure 1.** Suppression of fibroblast expression of matrix metalloproteinase 3 (MMP-3) and monocyte chemoattractant protein 1 (MCP-1) by $p16^{INK4a}$. **A,** Rheumatoid arthritis synovial fibroblasts (RASFs) infected with $p16^{INK4a}$ or control adenovirus were stimulated for 24 hours with interleukin-1$\beta$ (IL-1$\beta$) plus tumor necrosis factor $\alpha$ (TNF$\alpha$), and $^3$H-thymidine incorporation was assessed 3 days later (left). Mean reduction in $^3$H-thymidine incorporation induced by $p16^{INK4a}$ was 83% compared with controls. Flow cytometry showed an increase in cells at $G_0/G_1$ phase in RASFs expressing $p16^{INK4a}$ (right). Results are from 1 of 3 samples. **B,** RASFs infected with $p16^{INK4a}$ or control adenovirus were stimulated for 24 hours with IL-1$\beta$ plus TNF$\alpha$, and MMP-3, MCP-1, macrophage inflammatory protein 3$\alpha$ (MIP-3$\alpha$), and IL-6 in culture supernatants were measured by enzyme-linked immunosorbent assay. Mean reduction in MMP-3 and MCP-1 induced by $p16^{INK4a}$ was 78% and 91%, respectively, and mean reduction in MIP-3$\alpha$ and IL-6 production induced by $p21^{Cip1}$ was 69% and 67%, respectively, compared with controls. **C,** Adult normal human dermal fibroblasts (NHDF-Ad) and osteoarthritis synovial fibroblasts (OASFs) infected with $p16^{INK4a}$ or control adenovirus were stimulated for 24 hours with IL-1$\beta$ plus TNF$\alpha$, and the production of MMP-3 and MCP-1 was determined as in **B. D,** RNA from RASFs infected with $p16^{INK4a}$ or control adenovirus was examined for IL-1 receptor type I (IL-1RI) and GAPDH mRNA expression by Northern blotting. Mean reduction in IL-1RI mRNA expression induced by $p21^{Cip1}$ was 71% compared with controls. **E,** Whole cell extracts from RASFs infected with $p16^{INK4a}$ or $p18^{INK4c}$ adenovirus (Ad) were immunoprecipitated (IP) with anti-JNK antibody ($\alpha$-JNK) or control IgG and analyzed by Western blotting using antibodies specific for each cyclin-dependent kinase inhibitor: anti-$p16^{INK4a}$ ($\alpha$-p16), anti-$p18^{INK4c}$ ($\alpha$-p18), and anti-$p21^{Cip1}$ ($\alpha$-p21). Results are from 1 of 2 samples. **F,** RASFs infected with $p16^{INK4a}$ or control adenovirus were stimulated for 24 hours with IL-1$\beta$ plus TNF$\alpha$, and the DNA binding activities of activator protein 1 (AP-1), NF-$\kappa$Bp50, and NF-$\kappa$Bp65 were determined by colorimetric assay. Values are the mean and SD of 5 wells in **A,** 3 samples in **B** and **D,** 3 experiments in **C,** and triplicate cultures in **F.** * = $P < 0.05$; ** = $P < 0.01$. Data from previous experiments (8) showing the effects of $p21^{Cip1}$ (AxCAp21 adenovirus) on the proliferation of MIP-3$\alpha$ and IL-6 (**B**) and on IL-1RI mRNA expression (**D**) are also shown.

RASFs was 74 ± 37% and 101 ± 32%, respectively (mean ± SD). Thus, the production of these mediators of inflammation was not significantly affected by simple infection with control adenovirus.

Suppression of the release of mediators of inflammation by $p21^{Cip1}$ should be at least partly attributable to a down-regulation of IL-1RI expression (8). However, IL-1RI mRNA expression was not appreciably reduced in RASFs expressing $p16^{INK4a}$ as compared with RASFs infected with control adenovirus (Figure 1D). In addition, we and other investigators (8–10) have shown that $p21^{Cip1}$ associates with JNK to reduce JNK enzymatic activity. We further demonstrated previously that the DNA binding activity of AP-1, which is downstream of the JNK pathway, was reduced in RASFs expressing $p21^{Cip1}$ (8). This prompted us to examine $p16^{INK4a}$ for binding with JNK. Cell lysates of RASFs infected with AxCAp16 or AxCAp21 adenoviruses containing the human $p21^{Cip1}$ gene were immunoprecipitated with anti-$p16^{INK4a}$ or anti-$p21^{Cip1}$ antibody. Subsequent immunoblotting revealed that $p21^{Cip1}$, but not $p16^{INK4a}$, was associated with JNK (Figure 1E). Unlike $p21^{Cip1}$, $p16^{INK4a}$ did not appreciably inhibit AP-1 or NF-κB DNA binding activities in RASFs stimulated with inflammatory cytokines (Figure 1F). These data show that $p16^{INK4a}$ does not depend upon the suppression of JNK pathways or the down-regulation of IL-1RI expression for inhibition of the production of mediators of inflammation.

**Suppression of RASF expression of MMP-3 and MCP-1 by $p18^{INK4c}$.** The molecule $p18^{INK4c}$ is another member of the INK4 family of CDKIs that specifically inhibits CDK-4/6. Like $p16^{INK4a}$, this molecule did not bind to JNK (Figure 1D). It was not expressed by cultured RASFs, which were subsequently infected with Ad-RGD-p18 adenovirus containing a human $p18^{INK4c}$ gene or with control adenovirus. RASFs that expressed $p18^{INK4c}$ incorporated less $^3$H-labeled thymidine than did the controls (Figure 2A). Flow cytometric analyses revealed that cell cycle progression was inhibited at the $G_0/G_1$ phase in $p18^{INK4c}$-expressing RASFs (Figure 2A). ELISA of the culture supernatants showed that $p18^{INK4c}$ gene transfer down-regulated MMP-3 and MCP-1 production by RASFs (Figure 2B). These results show that $p16^{INK4a}$ and $p18^{INK4c}$ had the same effect and suggest that inhibition of CDK-4/6 activity should account for the suppression.

**Suppression of RASF production of mediators of inflammation by a small-molecule CDK-4/6 inhibitor.** A common function of $p16^{INK4a}$, $p18^{INK4c}$, and $p21^{Cip1}$ is to interact with cyclin D–CDK-4/6 complexes to suppress

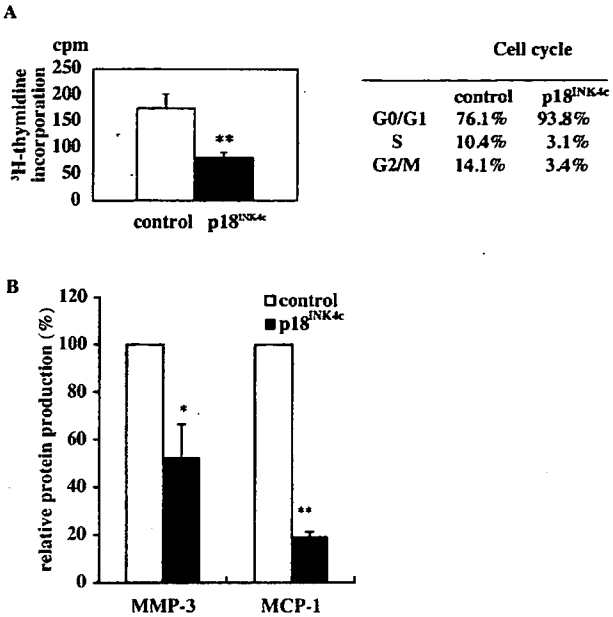


**Figure 2.** Suppression of RASF production of MMP-3 and MCP-1 by $p18^{INK4c}$. **A,** RASFs infected with $p18^{INK4c}$ or control adenovirus were stimulated with IL-1β plus TNFα, and $^3$H-thymidine incorporation was assessed (left). Mean reduction in $^3$H-thymidine incorporation induced by $p18^{INK4c}$ was 43% compared with controls. Flow cytometry showed an increase in cells at $G_0/G_1$ phase in RASFs expressing $p18^{INK4c}$ (right). Results are from 1 of 3 samples. **B,** RASFs infected with $p18^{INK4c}$ or control adenovirus were stimulated with IL-1β plus TNFα, and MMP-3 and MCP-1 in culture supernatants were measured by enzyme-linked immunosorbent assay. Mean reduction in MMP-3 and MCP-1 production induced by $p18^{INK4c}$ was 48% and 71%, respectively, compared with controls. Values are the mean and SD of 5 wells in A and 3 samples in B. * = $P < 0.05$; ** = $P < 0.01$. See Figure 1 for definitions.

CDK-4/6 activity. To examine whether inhibition of cyclin D–CDK-4/6 activity per se suppresses the production of mediators of inflammation by RASFs, we used CDK4I, a synthetic compound that specifically inhibits CDK-4/6. CDK4I inhibited $^3$H-thymidine incorporation by cytokine-stimulated RASFs in a dose-dependent manner. Even at the highest concentration examined, the number of cells in the $G_0/G_1$ phase of the cell cycle was increased without losing cell viability (Figure 3A). The amounts of MMP-3 and MCP-1 protein produced by RASFs treated with CDK4I were significantly less than those produced by controls (Figure 3B).

**Up-regulation of cell proliferation and RASF expression of MMP-3 by augmented CDK-4 activity.** We next augmented the activity of CDK-4/6 to study its effects on the production of mediators of inflammation.

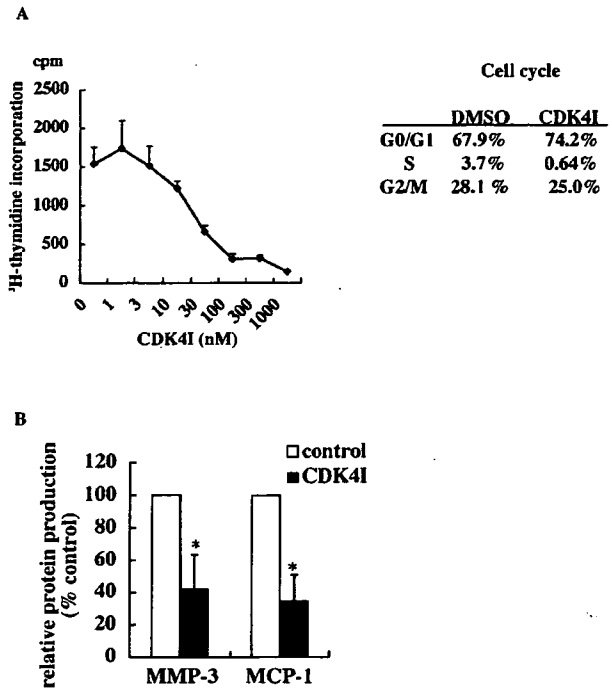


**Figure 3.** Suppression of RASF production of MMP-3 and MCP-1 by CDK4I, a small-molecule cyclin-dependent kinase 4/6 inhibitor. **A,** RASFs were treated for 12 hours with the indicated concentrations of CDK4I, stimulated with IL-1$\beta$ plus TNF$\alpha$, and $^3$H-labeled thymidine incorporation was assessed (left). Flow cytometry showed an increase in cells at $G_0/G_1$ phase in RASFs treated with 1 $\mu M$ CDK4I compared with control (DMSO) (right). Results are from 1 of 2 independent experiments. **B,** RASFs were treated with 1 $\mu M$ CDK4I or 0.5% DMSO (controls), stimulated with IL-1$\beta$ and TNF$\alpha$, and MMP-3 and MCP-1 in culture supernatants were measured by enzyme-linked immunosorbent assay. Mean reduction in MMP-3 and MCP-1 production induced by CDK4I was 57% and 64%, respectively, compared with controls. Values in **A** and **B** are the mean and SD of 3 samples. * = $P < 0.05$. See Figure 1 for definitions.

Although CDK-4/6 activity in normal cells is controlled by the amount of cyclin D, gene transfer of cyclin D1 alone did not accelerate cell cycle progression (17). To promote the function of cyclin D that binds to intranuclear CDK-4, products of the cyclin D1 transgene were directed to nuclei by adding a minigene that encodes a nuclear localization signal (16). Cotransfer of the cyclin D1–NLS gene construct and the CDK-4 gene into RASFs by adenoviruses resulted in phosphorylation (i.e., inactivation) of RB. Cotransfer also up-regulated $^3$H-thymidine incorporation into cultured RASFs and decreased the number of cells in the $G_0/G_1$ phase (Figure 4A). Because of limited titers of the prepared adenoviruses, the culture supernatants were subjected to ELISA only for MMP-3. When RASFs overexpressing cyclin D1–NLS and CDK-4 were stimulated, they produced more MMP-3 than did stimulated RASFs infected with the control virus (Figure 4B). Thus, the level of MMP-3 expression correlated directly with the activity of CDK-4.

**Regulation of MMP-3 production, but not MCP-1 production, by CDK activity at the mRNA level.** Levels of mRNA for MMP-3 and MCP-1 in RASFs were studied to discern underlying molecular events. Real-time PCR analysis showed that the MMP-3 mRNA level was reduced in $p16^{INK4a}$-expressing RASFs, whereas no significant change was observed in the MCP-1 mRNA level (Figure 4C). These results were confirmed by Northern blot analysis, which revealed significant reduction of MMP-3 mRNA levels, but not MCP-1 mRNA levels, in the $p16^{INK4a}$-expressing RASFs (Figure 4D). Treatment of RASFs with CDK4I also reduced the levels of mRNA for MMP-3, but not MCP-1, in the activated RASFs (Figure 4E). Thus, the levels of mRNA for MCP-1 did not account for the decrease in the amount of secreted protein.

**No dependence of transcriptional control of MMP-3 on RB.** It has been reported that introduction of active (i.e., unphosphorylated) RB suppresses the production of MMP-1, another tissue-degrading enzyme involved in rheumatoid inflammation, at the posttranscriptional level (27). Because mRNA levels of MMP-3 and MCP-1 were differentially controlled by CDK activity, we next investigated the regulation of these 2 molecules by RB. To manipulate the function of RB, which is the major substrate of CDK-4/6, we used a mutant RB gene that had replacement mutations at some of the phosphorylation sites. Adenoviral introduction of this gene increased the active, unphosphorylated form of RB, thus mimicking the suppression of the CDK-dependent phosphorylation of RB (18). We found that when RASFs overexpressed the active RB, they incorporated less $^3$H-thymidine as compared with control RASFs (Figure 5A). Flow cytometric analysis of the cell cycle showed that the active RB stopped their cell cycle at the $G_0/G_1$ phase (Figure 5A).

ELISA analyses of the culture supernatants showed that the production of both MMP-3 and MCP-1 was reduced in RASFs expressing the active RB (Figure 5B). Real-time PCR analysis revealed that MMP-3 and MCP-1 mRNA expression in RASFs overexpressing the active RB was preserved in comparison with the control RASFs (Figure 5C).

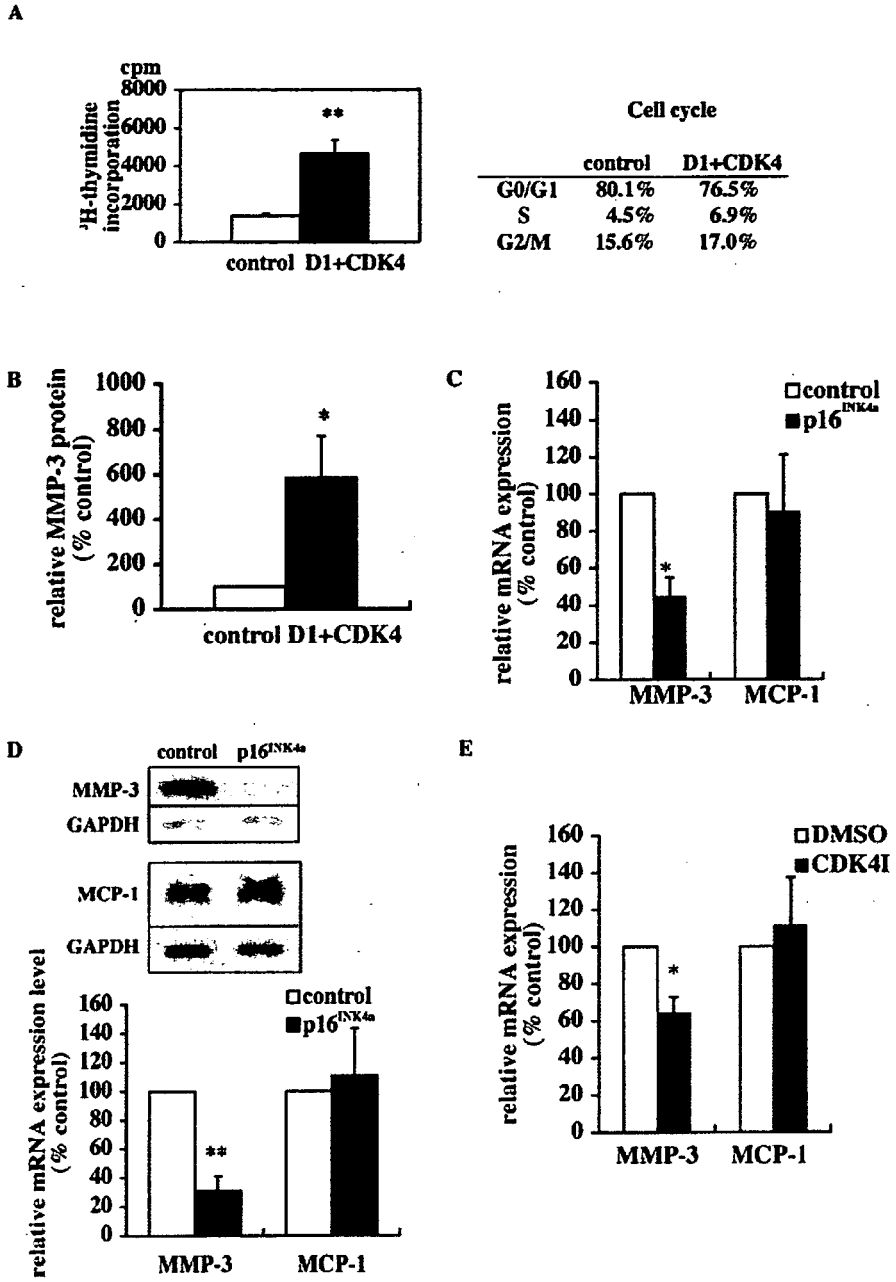


**Figure 4.** Effects of the combination of cyclin D1–nuclear localization signal (NLS) and cyclin-dependent kinase 4 (CDK-4) gene transfer on RASFs. **A,** RASFs were infected with cyclin D1–NLS plus CDK-4 (D1+CDK-4) or control adenovirus, and $^3$H-thymidine incorporation was assessed 60 hours later (left). Mean increase in RASFs was 240% compared with controls. Flow cytometry showed a decrease in cells at $G_0/G_1$ phase in RASFs expressing cyclin D1–NLS plus CDK-4 compared with control (right). Results are from 1 of 2 independent samples. **B,** RASFs infected with cyclin D1–NLS plus CDK-4 or control adenovirus and MMP-3 in culture supernatants was measured by enzyme-linked immunosorbent assay. Mean increase in RASFs was 490% compared with controls. **C–E,** RASFs infected with $p16^{INK4a}$ or control adenovirus (**C** and **D**) or treated with 1 $\mu M$ CDK4I or DMSO (control) (**E**) were stimulated with IL-1$\beta$ plus TNF$\alpha$, and MMP-3 and MCP-1 mRNA were analyzed by real-time polymerase chain reaction (**C** and **E**) or Northern blotting (**D**). Northern blotting results are from 1 of 3 samples. Levels of mRNA were standardized against GAPDH mRNA. Mean reduction in MMP-3 production induced by $p16^{INK4a}$ and by CDK4I was 56% (**C**), 70% (**D**), and 36% (**E**) compared with controls. Values are the mean and SD of 5 wells in **A** and 3 samples in **B–E**. * = $P < 0.05$; ** = $P < 0.01$. See Figure 1 for other definitions.

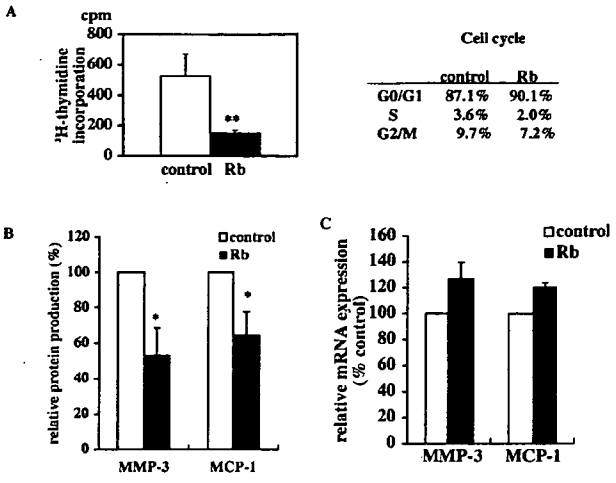


**Figure 5.** Suppression of RASF expression of MMP-3 and MCP-1 by constitutively active retinoblastoma (RB). **A,** RASFs were infected with nonphosphorylatable RB or control adenovirus, stimulated with IL-1$\beta$ plus TNF$\alpha$, and $^3$H-thymidine incorporation was assessed (left). Results are from 1 of 2 samples. Flow cytometry showed an increase in cells at $G_0/G_1$ phase in RASFs expressing the constitutively active RB (right). Results are from 1 of 2 independent samples. **B,** RASFs infected with the constitutively active RB or control adenovirus were stimulated for 24 hours with IL-1$\beta$ plus TNF$\alpha$, and MMP-3 and MCP-1 in culture supernatants were measured by enzyme-linked immunosorbent assay. Mean reduction in MMP-3 and MCP-1 production induced by RB was 48% and 36%, respectively, compared with controls. **C,** RASFs infected with RB or control adenovirus were stimulated with IL-1$\beta$ plus TNF$\alpha$, and mRNA for MMP-3 (**C**) and MCP-1 (**D**) was analyzed by real-time polymerase chain reaction. The mRNA levels are standardized against those of GAPDH. Values are the mean and SD of 5 wells in **A** and 3 samples in **B** and **C**. * = $P <$ 0.05; ** = $P < 0.01$. See Figure 1 for other definitions.

## DISCUSSION

The present study revealed that CDK-4/6 activity controls the production of MMP-3 by RASFs in a RB-independent manner. The regulation occurs at the mRNA level. RB, which is a substrate of CDK-4/6, can also regulate the expression of MCP-1 as well as MMP-3 at the posttranscriptional level (Figure 6). These features were not seen in control synovial or dermal fibroblasts that were not derived from an inflammatory milieu. Although the RA patients had been treated with various DMARDs, the reactivity of their fibroblasts was similar. We thus assume that the observed regulation is the result of an aberrant activation of the synovial fibroblasts in the rheumatoid joint rather than an intrinsic character of the RASFs or modification by therapeutic agents. The only functional CDK-4/6 substrate known at present is RB, which regulates the functional availability of E2F transcription factors for cell cycle progression. Our results predict the presence of other associating molecules that modulate the production of MMP-3 mRNA.

Bradley et al (27) reported that the phosphorylation status of RB correlates with the production of MMP-1 and IL-6. They showed that unphosphorylated RB suppresses expression of MMP-1 at the posttranscriptional level, and they suggested that this suppression is mediated by inhibition of p38 kinase. We found that a similar regulation is operative during the translation of MMP-3 and MCP-1. However, RB-independent control seems to dominate the regulation of MMP-3 production because it works at the mRNA level. Also, it was noted that CDK-inhibiting molecules suppressed MMP-3 production no less effectively than did the active RB (Figures 3B and 5B).

We have previously reported that $p21^{Cip1}$ could regulate mediators of inflammation in a CDK- independent manner (8). In the present study, we show that both CDK and its substrate RB can regulate them independently. Thus, cell cycle proteins are closely associated with the expression of inflammatory molecules through multiple pathways. It might be interesting to speculate

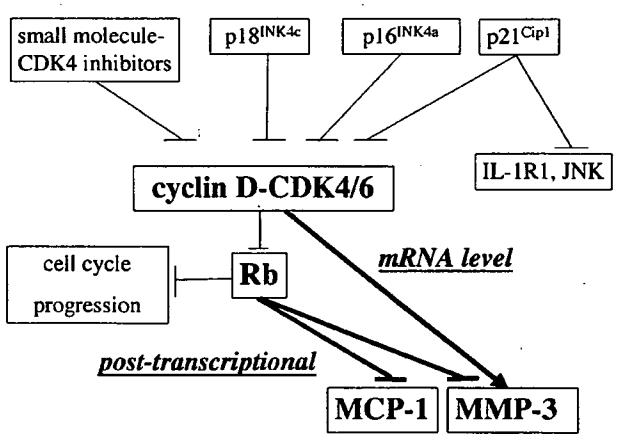


**Figure 6.** Multiple pathways of regulation of rheumatoid arthritis synovial fibroblast (RASF) production of mediators of inflammation by proteins of the cyclin-dependent kinase (CDK)–retinoblastoma (RB) axis. Inhibition of cyclin D–CDK-4/6 activity by p16$^{INK4a}$, p18$^{INK4c}$, or small-molecule CDK-4 inhibitors suppresses the production of matrix metalloproteinase 3 (MMP-3) and monocyte chemoattractant protein 1 (MCP-1) by RASFs. Inhibition of CDK-4/6 suppresses MMP-3 mRNA, but not MCP-1 mRNA. Active RB reduces the expression of MMP-3 and MCP-1 by posttranscriptional regulation. We have also previously found that $p21^{Cip1}$ can exert antiinflammatory effects outside the CDK–RB axis (8). IL-1RI = type I interleukin-1 receptor.

that unknown evolutional selections have imposed secure control of inflammation by cell cycle regulators.

MMP-3 degrades proteoglycans, gelatins, fibronectins, and collagens. Since it also activates other MMPs, it is the master proteinase in the cascade of tissue-degrading enzymes in the rheumatoid joint (28–30). Moreover, MMP-3 was found to be essential for joint destruction in an animal model of RA (31). In other models of RA, administration of MMP inhibitors that suppress the proteinases that are activated by MMP-3 prevented joint destruction (32–34). MCP-1 evokes both the migration and activation of lymphocytes and macrophages in RA synovial tissues (35). Administration of an MCP-1 antagonist was shown to be an effective treatment in an animal model of RA (36). Thus, mediators of inflammation that are down-regulated by the inhibition of CDK-4/6 play important roles in the inflammation that occurs in RA. Nevertheless, $p16^{INK4a}$ did not completely abrogate the production of MMP-3 and MCP-1. IL-1$\beta$– and TNF$\alpha$-stimulated RASFs expressing $p16^{INK4a}$ produced more mediators of inflammation than did unstimulated RASFs. We assume that the antiinflammatory effects of CDK-4/6 inhibition might assist the antiproliferative, therapeutic effects of CDKI in CDKI gene therapy.

In HeLa cells, $p16^{INK4a}$ interacts with NF-$\kappa$B to inhibit its transcriptional activity (37). Our preliminary studies suggest that $p16^{INK4a}$ in RASFs can regulate the expression of other cytokines in a CDK-4/6–independent manner. However, we found that overexpression of $p16^{INK4a}$ in RASFs did not suppress AP-1 and NF-$\kappa$B DNA binding activities. Since the Ets family transcription factors Ets-1 and Ets-2 up-regulate the expression of MMP-3, their suppression might account for the down-regulation of MMP-3 expression (38,39).

We showed that $p16^{INK4a}$, $p18^{INK4c}$, and $p21^{Cip1}$ gene transfer into RASFs can suppress their production of mediators of inflammation and proteinases via inhibition of CDK-4/6 activity. A small-molecule CDKI compound also down-regulated the expression of these molecules. For clinical application, modulation of cyclin–CDK activity by small-molecule CDK inhibitors is more feasible than CDKI gene transfer. Many small-molecule CDK inhibitors have already been developed and tested as oncostatics in clinical trials (40), and they might prove useful in the treatment of RA. However, since inhibition of the inflammatory molecules could also be independent of RB, each inhibitor may have a unique balance of the RB-dependent antiproliferative and RB-independent antiinflammatory effects. Thus, in the treatment of RA patients with CDK inhibitors, the two effects need to be balanced.

## ACKNOWLEDGMENTS

We thank Drs. T. Muneta, Y. Kuga, K. Taniguchi, J. Hasegawa, and K. Gotoh for providing synovial samples, Drs. N. Terada, M. Ikeda, J. M. Leiden, and E. Hatano for providing recombinant adenoviruses, Dr. C. Labrie for the $p18^{INK4c}$ plasmid, Dr. H. Mizuguchi for the recombinant adenoviral plasmids and technical advice, Genofunction, Inc. (Tsukuba, Japan) for constructing the $p18^{INK4c}$ adenovirus, and H. Mitsunaga and M. Toyomoto for technical assistance.

## REFERENCES

1. Arend WP. Physiology of cytokine pathways in rheumatoid arthritis. Arthritis Rheum 2001;45:101–6.
2. Bresnihan B. Pathogenesis of joint damage in rheumatoid arthritis. J Rheumatol 1999;26:17–719.
3. Andreakos E, Foxwell B, Brennan F, Maini R, Feldmann M. Cytokines and anti-cytokine biologicals in autoimmunity: present and future. Cytokine Growth Factor Rev 2002;13:299–313.
4. Taniguchi K, Kohsaka H, Inoue N, Terada Y, Ito H, Hirokawa K, et al. Induction of the p16INK4a senescence gene as a new therapeutic strategy for the treatment of rheumatoid arthritis. Nat Med 1999;5:760–7.
5. Nasu K, Kohsaka H, Nonomura Y, Terada Y, Ito H, Hirokawa K, et al. Adenoviral transfer of cyclin-dependent kinase inhibitor genes suppresses collagen-induced arthritis in mice. J Immunol 2000;165:7246–52.
6. Nonomura Y, Kohsaka H, Nasu K, Terada Y, Ikeda M, Miyasaka N. Suppression of arthritis by forced expression of cyclin-dependent kinase inhibitor $p21^{Cip1}$ gene into the joints. Int Immunol 2001;13:723–31.
7. Sherr CJ, Roberts JM. CDK inhibitors: positive and negative regulators of G1-phase progression. Genes Dev 1999;13:1501–12.
8. Nonomura Y, Kohsaka H, Nagasaka K, Miyasaka N. Gene transfer of a cell cycle modulator exerts anti-inflammatory effects in the treatment of arthritis. J Immunol 2003;171:4913–19.
9. Shim J, Lee H, Park J, Kim H, Choi EJ. A non-enzymatic p21 protein inhibitor of stress-activated protein kinases. Nature 1996; 381:804–6.
10. Perlman H, Bradley K, Liu H, Cole S, Shamiyeh E, Smith RC, et al. IL-6 and matrix metalloproteinase-1 are regulated by the cyclin-dependent kinase inhibitor p21 in synovial fibroblasts. J Immunol 2003;170:838–45.
11. Arnett FC, Edworthy SM, Bloch DA, McShane DJ, Fries JF, Cooper NS, et al. The American Rheumatism Association 1987 revised criteria for the classification of rheumatoid arthritis. Arthritis Rheum 1988;31:315–24.
12. Terada Y, Yamada T, Nakashima O, Tamamori M, Ito H, Sasaki S, et al. Overexpression of cell cycle inhibitors ($p16^{INK4a}$ and $p21^{Cip1}$) and cyclin D1 using adenovirus vectors regulates proliferation of rat mesangial cells. J Am Soc Nephrol 1997;8:51–60.
13. Blais A, Labrie Y, Pouliot F, Lachance Y, Labrie C. Structure of the gene encoding the human cyclin-dependent kinase inhibitor p18 and mutational analysis in breast cancer. Biochem Biophys Res Commun 1998;247:146–53.
14. Mizuguchi H, Kay MA. A simple method for constructing E1- and E1/E4-deleted recombinant adenoviral vectors. Hum Gene Ther 1999;10:2013–7.
15. Mizuguchi H, Kay MA. Efficient construction of a recombinant

adenovirus vector by an improved in vitro ligation method. Hum Gene Ther 1998;9:2577–83.
16. Tamamori-Adachi M, Ito H, Nobori K, Hayashida K, Kawauchi J, Adachi S, et al. Expression of cyclin D1 and CDK4 causes hypertrophic growth of cardiomyocytes in culture: a possible implication for cardiac hypertrophy. Biochem Biophys Res Commun 2002;296:274–80.
17. Tamamori-Adachi M, Ito H, Sumrejkanchanakij P, Adachi S, Hiroe M, Shimizu M, et al. Critical role of cyclin D1 nuclear import in cardiomyocyte proliferation. Circ Res 2003;92:e12–9.
18. Chang MW, Barr E, Seltzer J, Jiang YQ, Nabel GJ, Nabel EG, et al. Cytostatic gene therapy for vascular proliferative disorders with a constitutively active form of the retinoblastoma gene product. Science 1995;267:518–22.
19. Terao R, Honda K, Hatano E, Uehara T, Yamamoto M, Yamaoka Y. Suppression of proliferative cholangitis in a rat model with direct adenovirus-mediated retinoblastoma gene transfer to the biliary tract. Hepatology 1998;28:605–12.
20. Mizuguchi H, Koizumi N, Hosono T, Utoguchi N, Watanabe Y, Kay MA, et al. A simplified system for constructing recombinant adenoviral vectors containing heterologous peptides in the HI loop of their fiber knob. Gene Ther 2001;8:730–5.
21. Inoue H, Takamori M, Nagata N, Nishikawa T, Oda H, Yamamoto S, et al. An investigation of cell proliferation and soluble mediators induced by interleukin 1β in human synovial fibroblasts: comparative response in osteoarthritis and rheumatoid arthritis. Inflamm Res 2001;50:65–72.
22. Elshaw SR, Henderson N, Knox AJ, Watson SA, Buttle DJ, Johnson SR. Matrix metalloproteinase expression and activity in human airway smooth muscle cells. Br J Pharmacol 2004;142: 1318–24.
23. Pierer M, Rethage J, Seibl R, Lauener R, Brentano F, Wagner U, et al. Chemokine secretion of rheumatoid arthritis synovial fibroblasts stimulated by Toll-like receptor 2 ligands. J Immunol 2004;172:1256–65.
24. Zhong H, Simons JW. Direct comparison of GAPDH, β-actin, cyclophilin, and 28S rRNA as internal standards for quantifying RNA levels under hypoxia. Biochem Biophys Res Commun 1999; 259:523–26.
25. Zhu G, Conner SE, Zhou X, Shih C, Li T, Anderson BD, et al. Synthesis, structure-activity relationship, and biological studies of indolocarbazoles as potent cyclin D1-CDK4 inhibitors. J Med Chem 2003;46:2027–30.
26. Patel R, Bartosch B, Blank JL. $p21^{WAF1}$ is dynamically associated with JNK in human T-lymphocytes during cell cycle progression. J Cell Sci 1998;111:2247–55.
27. Bradley K, Scatizzi JC, Fiore S, Shamiyeh E, Koch AE, Firestein GS, et al. Retinoblastoma suppression of matrix metalloproteinase 1, but not interleukin-6, through a p38-dependent pathway in rheumatoid arthritis synovial fibroblasts. Arthritis Rheum 2004;50: 78–87.
28. Okada Y. Proteinases and matrix degradation. In: Ruddy S, Harris ED Jr, Sledge CB, Budd RC, Sergent JS, editors. Kelley's textbook of rheumatology. 6th ed. Philadelphia: WB Saunders; 2001. p. 55–72.
29. Tolboom TC, Pieterman E, van der Laan WH, Toes RE, Huidekoper AL, Nelissen RG, et al. Invasive properties of fibroblast-like synoviocytes: correlation with growth characteristics and expression of MMP-1, MMP-3, and MMP-10. Ann Rheum Dis 2002;61: 975–80.
30. Nagase H. Activation mechanisms of matrix metalloproteinases. Biol Chem 1997;378:151–60.
31. Van Meurs J, van Lent P, Stoop R, Holthuysen A, Singer I, Bayne E, et al. Cleavage of aggrecan at the $Asn^{341}$-$Phe^{342}$ site coincides with the initiation of collagen damage in murine antigen-induced arthritis: a pivotal role for stromelysin 1 in matrix metalloproteinase activity. Arthritis Rheum 1999;42:2074–84.
32. Hamada T, Arima N, Shindo M, Sugama K, Sasaguri Y, Brewster M, et al. Suppression of adjuvant arthritis of rats by a novel matrix metalloproteinase-inhibitor Ro 32-3555, an orally active collagenase selective inhibitor, prevents structural damage in the STR/ ORT mouse model of osteoarthritis. Ro 32-3555, an orally active collagenase inhibitor, prevents cartilage breakdown in vitro and in vivo. Br J Pharmacol 2000;131:1513–20.
33. Ishikawa T, Nishigaki F, Miyata S, Hirayama Y, Minoura K, Imanishi J, et al. Prevention of progressive joint destruction in adjuvant induced arthritis in rats by a novel matrix metalloproteinase inhibitor, FR217840: suppression of adjuvant arthritis of rats by a novel matrix metalloproteinase-inhibitor. Eur J Pharmacol 2005;508:239–47.
34. Lewis EJ, Bishop J, Bottomley KM, Bradshaw D, Brewster M, Broadhurst MJ, et al. Ro 32-3555, an orally active collagenase inhibitor, prevents cartilage breakdown in vitro and in vivo. Br J Pharmacol 1997;121:540–6.
35. Koch AE, Kunkel SL, Harlow LA, Johnson B, Evanoff HL, Haines GK, et al. Enhanced production of monocyte chemoattractant protein-1 in rheumatoid arthritis. J Clin Invest 1992;90:772–9.
36. Gong JH, Ratkay LG, Waterfield JD, Clark-Lewis I. An antagonist of monocyte chemoattractant protein 1 (MCP-1) inhibits arthritis in the MRL-lpr mouse model. J Exp Med 1997;186:131–7.
37. Wolff B, Naumann M. INK4 cell cycle inhibitors direct transcriptional inactivation of NF-κB. Oncogene 1999;18:2663–6.
38. Wasylyk C, Gutman A, Nicholson R, Wasylyk B. The c-Ets oncoprotein activates the stromelysin promoter through the same elements as several non-nuclear oncoproteins. EMBO J 1991;10: 1127–34.
39. White LA, Maute C, Brinckerhoff CE. ETS sites in the promoters of the matrix metalloproteinases collagenase (MMP-1) and stromelysin (MMP-3) are auxiliary elements that regulate basal and phorbol-induced transcription. Connect Tissue Res 1997;36: 321–35.
40. Senderowicz AM. Small-molecule cyclin-dependent kinase modulators. Oncogene 2003;22:6609–20.

# Lipopolysaccharide-Induced Up-Regulation of Triggering Receptor Expressed on Myeloid Cells-1 Expression on Macrophages Is Regulated by Endogenous Prostaglandin $E_2$[1]

Yousuke Murakami,[2]* Hitoshi Kohsaka,*† Hidero Kitasato,‡ and Tohru Akahoshi§

**Triggering receptor expressed on myeloid cells-1 (TREM-1) is a recently identified cell surface molecule that is expressed by neutrophils and monocytes. TREM-1 expression is modulated by various ligands for TLRs in vitro and in vivo. However, the influence of $PGE_2$, a potential mediator of inflammation, on TREM-1 expression has not been elucidated. In this study, we examined the effects of $PGE_2$ on LPS-induced TREM-1 expression by resident murine peritoneal macrophages (RPM) and human PBMC. $PGE_2$ significantly induced murine TREM-1 (mTREM-1) expression by RPM. Up-regulation of TREM-1 expression was specific to $PGE_2$ among arachidonic acid metabolites, while ligands for chemoattractant receptor-homologous molecule expressed on Th2 cells and the thomboxane-like prostanoid receptor failed to induce mTREM-1 expression. $PGE_2$ also increased expression of the soluble form of TREM-1 by PBMC. LPS-induced TREM-1 expression was regulated by endogenous $PGE_2$ especially in late phase (>2 h after stimulation), because cyclooxygenase-1 and -2 inhibitors abolished this effect at that points. A synthetic EP4 agonist and 8-Br-cAMP also enhanced mTREM-1 expression by RPM. Furthermore, protein kinase A, PI3K, and p38 MAPK inhibitors prevented $PGE_2$-induced mTREM-1 expression by RPM. Activation of TREM-1 expressed on $PGE_2$-pretreated PBMC by an agonistic TREM-1 mAb significantly enhanced the production of IL-8 and TNF-$\alpha$. These findings indicate that LPS-induced TREM-1 expression on macrophages is mediated, at least partly, by endogenous $PGE_2$ followed by EP4 and cAMP, protein kinase A, p38 MAPK, and PI3K-mediated signaling. Regulation of TREM-1 and the soluble form of TREM-1 expression by $PGE_2$ may modulate the inflammatory response to microbial pathogens.** *The Journal of Immunology,* **2007, 178: 1144–1150.**

Triggering receptor expressed on myeloid cells-1 (TREM-1)[3] is a recently discovered cell surface molecule that has been identified on neutrophils and monocytes (1, 2). The soluble form of TREM-1 (sTREM-1) is detected in bronchoalveolar lavage fluid from patients with microbial infection and has been demonstrated to act as an inhibitor of TREM-1 (3–6). TREM-1 is a 30-kDa glycoprotein belonging to the Ig superfamily and its expression is up-regulated by various ligands for TLRs (7–9). Activation of TREM-1 expressed on neutrophils and monocytes by an agonistic mAb has been shown to stimulate the expression of various proinflammatory cytokines, chemokines, and cell surface molecules (1, 7–9). Furthermore, LPS causes synergistic enhancement of cytokine production by monocytes in response to the agonistic mAb, indicating that TREM-1 amplifies inflammatory responses initiated by TLRs (1, 7–9). Although the natural ligands for TREM-1 have not been identified, its essential role in acute inflammatory responses has been demonstrated in murine models of septic shock, because blocking of TREM-1 by a sTREM-1 improves the survival of mice with bacterial sepsis (6, 9). Thus, activation of TREM-1 may play a crucial role in the inflammatory response to microbes.

PGs are multipotent mediators that modulate a number of pathophysiological responses. PGs are produced by metabolism of arachidonic acid through activation of cyclooxygenase (COX). COX has two isoforms, which are COX-1 and COX-2 (10). COX-1 is constitutively expressed, whereas COX-2 is expressed at low level by most normal resting cells. COX-2 expression is induced by various TLR ligands (11, 12) and release of PGs is significantly increased in various animal models of endotoxemia or sepsis (13, 14). In particular, $PGE_2$ has been shown to function as a mediator of sepsis-induced immunosuppression, an inhibitor of proinflammatory cytokine production by macrophages, and an inducer of IL-10 production (15). In contrast, $PGE_2$ has several detrimental effects in sepsis, including vasodilation and increased vascular permeability (16). Several previous studies have shown that COX inhibitors can improve the survival of mice after burn infection or administration of a lethal dose of LPS (17–19). These findings indicate that PGs play an important role in microbial inflammation, including sepsis or endotoxemia. However, the precise mechanisms by which PGs (particularly $PGE_2$) have a regulatory effect on microbial inflammation have not been determined.

Although TREM-1 is clearly induced by LPS, little is known regarding the biological influence of $PGE_2$ on TREM-1 during

*Research Unit for Clinical Immunology, RIKEN Research Center for Allergy and Immunology, Kanagawa, Japan; †Department of Medicine and Rheumatology, Tokyo Medical and Dental University, Tokyo, Japan; ‡Department of Microbiology, Kitasato University School of Allied Health Sciences, Kanagawa, Japan; and §Department of General Medicine, Kitasato University School of Medicine, Kanagawa, Japan

Received for publication September 13, 2005. Accepted for publication November 8, 2006.

The costs of publication of this article were defrayed in part by the payment of page charges. This article must therefore be hereby marked *advertisement* in accordance with 18 U.S.C. Section 1734 solely to indicate this fact.

[1] This work was supported in part by a research program of the Graduate School of Medical Sciences, Kitasato University, research grants from the Ministry of Education, Science, Sports and Culture of Japan, and research grants from the Ministry of Health, Labour and Welfare of Japan.

[2] Address correspondence and reprint requests to Dr. Yousuke Murakami, Clinical Immunology Unit, RIKEN Research Center for Allergy and Immunology, 1-7-22 Suehiro-cho, Tsurumi-ku, Yokohama City, Kanagawa, 230-0045, Japan. E-mail address: y-mura@rcai.riken.jp

[3] Abbreviations used in this paper: TREM, triggering receptor expressed on myeloid cells; mTREM, murine TREM; hTREM, human TREM; sTREM, soluble form of TREM; hsTREM, human sTREM; PKA, protein kinase A; COX, cyclooxygenase; RPM, resident peritoneal macrophage; I-BOP, 1*S*-[1$\alpha$,2$\alpha$(*Z*),3$\beta$(1*E*,3*S*),4$\alpha$]-7-[3-[3-hydroxy-4-(4-iodophenoxy)-1-butenyl]-7-oxabicyclo[2.2.1]hept-2-yl]-5-heptenoic acid; TP, thromboxane-like prostanoid; CRTH2, chemoattractant receptor-homologous molecule expressed on Th2 cells; EP, E-series of prostaglandin.

Table I. *Oligonucleotide primers and probes used for real-time PCR*

| Target Gene | Type[a] | Primer or Probe (5′–3′) | Description (mer) |
|---|---|---|---|
| mTREM-1 | F | CCAGAAGGCTTGGCAGAGACT | 22 |
| | B | ACTTCCCCATGTGGACTTCACT | 22 |
| mGAPDH | F | TGCAGTGGCAAAGTGGAGATT | 21 |
| | B | ATTTGCCGTGAGTGGAGTCAT | 21 |
| hTREM-1 | F | GCCTTGTGCCCACTCTATACCA | 22 |
| | B | TGGAGACATCGGCAGTTGAC | 20 |
| | P | (FAM)CAGAACTGTGACCCAAGCTCCACCCA(TAMRA) | 26 |
| hsTREM-1 | F | CCTCCCAAGGAGCCTCACA | 19 |
| | B | ACACCGGAACCCCTTGGT | 18 |
| | P | (FAM)CTGTTCGATCGCATCCGCTTGGT(TAMRA) | 23 |

[a] F, forward primer; B, backward primer; and P, TaqMan Probe.

microbial inflammation. Therefore, we conducted this study to investigate the biological effects of $PGE_2$ on the expression and action of TREM-1.

## Materials and Methods

### *Reagents*

DI-004 (an EP1 agonist), AE1–259-01 (an EP2 agonist), AE-248 (an EP3 agonist), and AE1-329 (an EP4 agonist) were provided by Ono Pharmaceuticals. A monoclonal rat anti-mouse TREM-1 Ab and a monoclonal mouse anti-human TREM-1 Ab, as well as control mouse IgG1 and a polyclonal anti-actin Ab, were obtained from R&D Systems and Santa Cruz Biotechnology, respectively. HRP-conjugated rabbit anti-mouse IgG and HRP-conjugated rabbit anti-rat IgG were purchased from DakoCytomation. Specific ELISAs for human TNF-$\alpha$ and human IL-8 were obtained from BioSource International. 8-Bromoadenosine 3′, 5′ cyclic monophosphate (8-Br-cAMP), LPS, the MEK (MAPKK) inhibitor PD98059, the p38 MAPK inhibitor SB203580, and the PI3K inhibitor LY294002 were purchased from Sigma-Aldrich, while the protein kinase A (PKA) inhibitor H-89 was obtained from Seikagaku. $PGD_2$, $PGE_2$, 1*S*-[1$\alpha$, 2$\alpha$(*Z*),3$\beta$(1*E*,3*S*),4$\alpha$]-7-[3-[3-hydroxy-4-(4-iodophenoxy)-1-butenyl]-7-oxabicyclo[2,2,1]hept-2-yl]-5-heptenoic acid (I-BOP), a COX-1 inhibitor (SC560), a COX-2 inhibitor (NS398), and a $PGE_2$ EIA kit were obtained from Cayman Chemical.

### *Cell culture*

Resident peritoneal macrophages (RPM) were isolated from male ICR mice (6–8 wk old) as reported elsewhere (15). Heparinized peripheral blood was obtained from healthy volunteers and human PBMC were isolated by density-gradient centrifugation with Ficoll-Paque. After washing with PBS, the RPM or PBMC were suspended in RPMI 1640 medium (Sigma-Aldrich) supplemented with 5% heat-inactivated FCS (HyClone), 100 U/ml penicillin, and 100 $\mu$g/ml streptomycin (Invitrogen Life Technologies) for culture under a 5% $CO_2$ atmosphere at 37°C.

RPM ($1 \times 10^6$ cells) or PBMC ($2 \times 10^6$ cells) were incubated for the indicated periods with or without various concentrations of PGs ($PGD_2$, $PGE_2$, I-BOP), 8-Br-cAMP, LPS, or E-series of prostaglandin (EP EP1–4) agonists. Then the expression of murine TREM-1 (mTREM-1), human TREM-1 (hTREM-1), and soluble hTREM-1 (hsTREM-1) was investigated.

RPM were incubated in the presence or absence of SC560 and/or NS398 for 1 h to inhibit endogenous COX activity, and then the cells were incubated in the presence of LPS for the indicated periods. To block protein kinase activity, RPM were incubated in the presence or absence of various inhibitors such as SB203580, PD98059, LY294002, or H89 for 30 min, after which the cells were incubated with LPS or $PGE_2$ for the indicated periods.

At the termination of incubation, cells and culture supernatants were obtained by centrifugation. Total RNA and protein were isolated by using RLT lysis buffer (Qiagen). Samples of cell lysate and culture medium were stored at −80°C until use.

### *Quantitative real-time PCR*

Total RNA was extracted from cell lysates using an RNeasy Mini kit (Qiagen). The RNA was treated with DNase I (Qiagen) and cDNA was synthesized from 2 $\mu$g of random-primed total RNA in a volume of 20 $\mu$l using Omniscript reverse transcriptase (Qiagen). mTREM-1, GAPDH, and COX-2 were assessed by quantitative real-time PCR (SYBR) using specific oligonucleotide primers. hTREM-1, hsTREM-1, and rRNA were assessed by quantitative real-time PCR (TaqMan) using specific oligonucleotide primers and probe. hsTREM-1 was identified as a splice variant of hTREM-1 with a 193-base deletion (exon 3) from bases 471 to 663 (GenBank accession no. AF287008). To avoid amplification of hsTREM-1 mRNA, the forward primer for hTREM-1 was designed to fit exon 3 (the deletion site). To amplify only hsTREM-1, the backward primer was designed to hybridize to the 3′ end of exon 2 as well as the 5′ end of exon 4. These primers could specifically amplify hTREM-1 and hsTREM-1, respectively. The sequences of the primers and probes are listed in Table I. The rRNA primers and probe were purchased from Applied Biosystems. The SYBR PCR was performed in duplicate using a 25-$\mu$l reaction mixture containing 1 $\mu$l of cDNA, QuantiTect SYBR Green PCR (Qiagen), and 300 nM each of the sense and antisense primers. The PCR mixture was incubated for 15 min at 95°C, and then amplification was performed for 45 cycles, consisting of denaturation at 94°C for 15 s, annealing at 58°C for 30 s, and extension at 72°C for 30 s. TaqMan PCR was performed in duplicate with a 25-$\mu$l reaction mixture containing 1 $\mu$l of cDNA, 12.5 $\mu$l of QuantiTect Probe PCR (Qiagen), 400 nM each of the sense and antisense primers, and 200 nM of the probe. The PCR mixture was incubated for 15 min at 95°C to activate HotStarTaq DNA polymerase. Subsequently, amplification was performed for 45 cycles, consisting of denaturation at 94°C for 15 s and combined annealing extension at 59°C for 1 min. During the extension step, the ABI Prism 7700 Sequence Detection System monitored PCR amplification in real time by quantitative analysis of the emitted fluorescence. The amount of each sample mRNA was evaluated relative to the control sample, which was assigned a value of 1 arbitrary unit.

### *Western blot analysis*

Culture medium or RPM ($1 \times 10^6$ cells) was dissolved in sample buffer (350 mM Tris (pH 6.8), 10% SDS, 30% glycerol, 600 mM DTT, and 0.05% bromphenol blue), loaded onto 10% SDS-PAGE gel, and run at 20 mA for 1.5 h. Proteins in the supernatant were transferred to a polyvinylidene difluoride membrane (Roche Diagnostics) for 1.5 h at 200 mA by semidry blotting. The membrane was then blocked with 5% skim milk in PBS containing 0.05% Tween 20 for 1 h at 37°C, washed with PBS containing 0.1% Tween 20, and incubated overnight at 4°C with a monoclonal anti-human TREM-1 Ab (1 $\mu$g/ml). The blots were washed four times with TBS and incubated for 30 min with HRP-conjugated rabbit anti-mouse IgG. Immunoreactive bands were developed using a chemiluminescent substrate (ECL plus; Amersham Biosciences).

### *Assay of cytokine and chemokine production*

Flat-bottom plates were precoated with 5 $\mu$g/ml of a monoclonal anti-human TREM-1 Ab or an isotype-matched control Ab (mouse IgG1) overnight at 4°C. After washing with PBS, PBMC ($1 \times 10^5$ cells) were preincubated with or without $PGE_2$ (1 $\mu$M) for 5 h. Then the PBMC were added to the Ab-coated wells, and briefly spun in a centrifuge at 1200 rpm to bind TREM-1. After incubation for 24 h, culture medium was obtained by centrifugation and stored at −20°C until the levels of TNF-$\alpha$ and IL-8 in the supernatant were determined by specific ELISAs.

### *Assay of $PGE_2$ production*

Concentration of $PGE_2$ in the culture supernatant was determined by using a $PGE_2$ EIA kit according to the manufacturer's instructions.

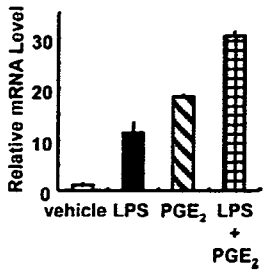


**FIGURE 1.** $PGE_2$ and LPS up-regulate mTREM-1 expression by RPM. RPM were incubated with or without $PGE_2$ (1 $\mu$M) for 1 h, and then were cultured in the presence or absence of LPS (100 ng/ml). The mTREM-1 mRNA level was determined by quantitative real-time PCR using murine GAPDH as the internal control. The relative level of mTREM-1 mRNA was evaluated by comparison with that in vehicle (EtOH)-treated RPM, which was defined as 1 arbitrary unit. Data are expressed as the mean ± SD of triplicate determinations.

*Statistical analysis*

Results are expressed as the mean ± SD. Statistical analysis was performed using the paired Student $t$ test and $p < 0.05$ was considered to indicate significance.

## Results

*$PGE_2$ induces TREM-1 expression by RPM*

$PGE_2$ is a mediator with a wide variety of biological effects in the process of microbial inflammation. To determine whether $PGE_2$ could influence the expression and action of TREM-1 in macrophages, RPM were pretreated with $PGE_2$ at a concentration of 1 $\mu$M for 1 h and then the cells were subsequently incubated in the presence or absence of LPS (100 ng/ml) for 1 h. Expression of mTREM-1 was determined by quantitative real-time PCR. LPS significantly increased expression of the *TREM-1* gene (Fig. 1), as previously reported. $PGE_2$ also caused significant induction of TREM-1 expression and the magnitude of gene expression was significantly higher in $PGE_2$-treated cells than in LPS-treated cells. Furthermore, a combination of $PGE_2$ and LPS caused additive enhancement of mTREM-1 expression by RPM.

To investigate the time course of $PGE_2$-induced expression of mTREM-1, RPM were incubated with 1 $\mu$M $PGE_2$ for the indicated periods. Induction of gene expression occurred quite rapidly and was observed as early as 1 h after stimulation, following declined for 12 h (Fig. 2*A*). RPM were incubated with varying concentrations of $PGE_2$ for 1 h to determine whether physiological levels of $PGE_2$ enhanced mTREM-1 expression. It was shown that $PGE_2$ increased mTREM-1 expression in a concentration-dependent manner. $PGE_2$ at a concentration as low as $10^{-10}$ M significantly induced mTREM-1 expression and maximal expression occurred after stimulation with $10^{-6}$–$10^{-7}$ M $PGE_2$ (Fig. 2*B*).

It has been demonstrated that monocytes and macrophages express various receptors for arachidonic acid metabolites, which are referred to EP, thromboxane-like prostanoid (TP), and CRTH2 (20). Therefore, we investigated the effects of specific ligands for these receptors on mTREM-1 expression by RPM. The cells were incubated for 1 h with $PGE_2$ (an EP receptor ligand), I-BOP (a TP receptor ligand), or $PGD_2$ (a CRTH2 ligand), and TREM-1 expression was evaluated by quantitative real-time PCR. $PGE_2$ induced TREM-1 expression, while neither I-BOP nor $PGD_2$ up-regulated mTREM-1 expression, indicating that $PGE_2$ was a specific inducer of mTREM-1 expression among these PGs (Fig. 2*C*).

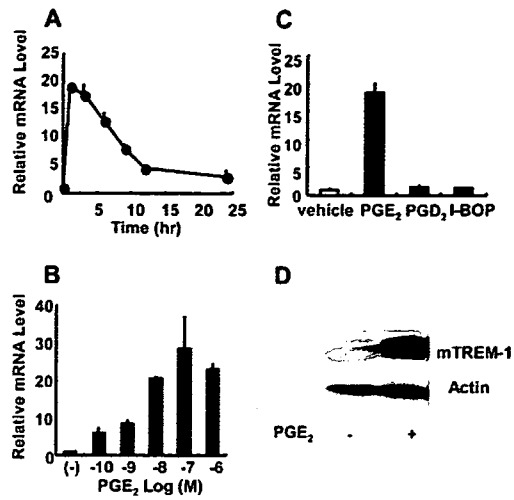


**FIGURE 2.** $PGE_2$ induces mTREM-1 expression in a time- or concentration-dependent manner. *A*, RPM were incubated with $PGE_2$ (1 $\mu$M) for the indicated periods and the mTREM-1 mRNA level was determined by quantitative real-time PCR. *B*, RPM were cultured with or without various concentrations of $PGE_2$ for 1 h and the mTREM-1 mRNA level was determined by quantitative real-time PCR. *C*, RPM were incubated with $PGE_2$ (1 $\mu$M), $PGD_2$ (1 $\mu$M), or I-BOP (0.2 $\mu$M) for 1 h and the mTREM-1 mRNA level was determined by quantitative real-time PCR. *D*, RPM were cultured with or without $PGE_2$ (1 $\mu$M) for 5 h, and expression of mTREM-1 protein and actin was determined by Western blot analysis. Data are expressed as the mean ± SD of triplicate determinations.

Western blot analysis using a specific anti-mouse TREM-1 mAb was performed to evaluate mTREM-1 protein expression by RPM after incubation with or without $PGE_2$ for 5 h. mTREM-1 protein was detected faintly when RPM were incubated with the vehicle alone, whereas increased expression of mTREM-1 was clearly seen when RPM were incubated with $PGE_2$ ($10^{-6}$ M) for 5 h (Fig. 2*D*).

*Endogenous $PGE_2$ induces TREM-1 expression by RPM*

It has been demonstrated that LPS induces TREM-1 expression as well as the release of $PGE_2$ by macrophages (7–9, 21). To evaluate the possible influence of endogenous $PGE_2$ on LPS-induced mTREM-1 expression, RPM were stimulated with LPS (100 ng/ml) for the indicated periods, after which $PGE_2$ production and *mTREM-1* gene expression were determined by EIA and quantitative real-time PCR, respectively. $PGE_2$ synthesis gradually increased up to 4 h, and then the maximum level was maintained

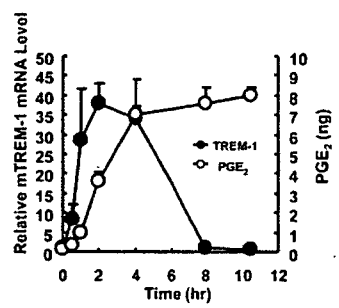


**FIGURE 3.** LPS-induced $PGE_2$ production up-regulates mTREM-1 expression by RPM. RPM were stimulated with LPS (100 ng/ml) for the indicated periods. Then the mTREM-1 mRNA level was determined by quantitative real-time PCR, and $PGE_2$ synthesis was determined by using a $PGE_2$ EIA kit. Data are expressed as the mean ± SD of triplicate determinations.

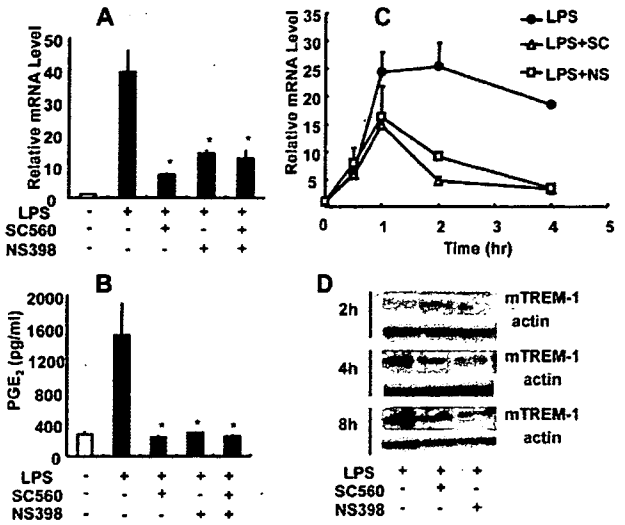


**FIGURE 4.** Effect of COX inhibitors on LPS-induced mTREM-1 expression by RPM. RPM were pretreated with or without SC560 and/or NS398 for 1 h, and were subsequently incubated in the presence or absence of LPS (100 ng/ml) for the indicated periods. *A*, The mTREM-1 mRNA level at 2 h after LPS stimulation was determined by quantitative real-time PCR. *B*, $PGE_2$ synthesis at 2 h after LPS stimulation was determined by a $PGE_2$ EIA kit. *C*, Time course of mTREM-1 mRNA expression was determined by quantitative real-time PCR. *D*, mTREM-1 protein and actin was determined by Western blot analysis. Data are expressed as the mean ± SD of triplicate determinations. *, $p < 0.01$, vs LPS-stimulated RPM by Student's unpaired *t* test.

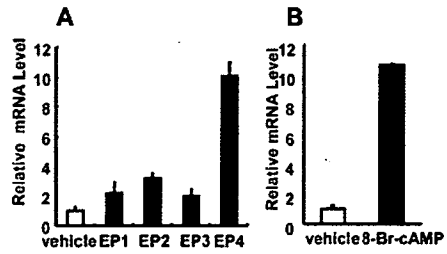


**FIGURE 5.** Enhancement of mTREM-1 expression by an EP4 agonist and cAMP analog. *A*, RPM were incubated with or without agonists for EP1 to EP4 agonists (1 μM) for 1 h and the mTREM-1 mRNA level was determined by quantitative real-time PCR. *B*, RPM were incubated with or without 8-Br-cAMP (0.5 mM) for 1 h. Data are expressed as the mean ± SD of triplicate determinations.

until 11 h after stimulation (Fig. 3). In contrast, gene expression of mTREM-1 occurred quite rapidly and was seen as early as 0.5 h after stimulation when $PGE_2$ production was not detected. Maximum induction of mTREM-1 was observed at 2–4 h after stimulation and gene expression returned to the basal level by 8 h. These findings indicated that $PGE_2$ synthesis did not precede the induction of *mTREM-1* gene expression.

mTREM-1 expression was significantly induced by a physiological concentration of $PGE_2$. Therefore, the regulatory roles of $PGE_2$ on TREM-1 expression was investigated. Because $PGE_2$ synthesis is regulated by COX-1 and COX-2, RPM were incubated for 1 h in the presence or absence of SC560 (a selective COX-1 inhibitor) or NS398 (a selective COX-2 inhibitor), and then the cells were stimulated with LPS for 2 h. mTREM-1 expression and $PGE_2$ synthesis was determined by quantitative real-time PCR and EIA, respectively. Both inhibitors for COX-1 and COX-2 partially, but significantly, inhibited LPS-induced expression of mTREM-1 (Fig. 4*A*). When the effects of COX inhibitors on $PGE_2$ synthesis by LPS-stimulated RPM were investigated, these inhibitors also suppressed $PGE_2$ synthesis (Fig. 4*B*). Vehicle (DMSO) did not affect on LPS-induced $PGE_2$ synthesis and mTREM-1 expression (data not shown).

To investigate the effect of $PGE_2$ on LPS-induced mTREM-1 mRNA expression at early time points, RPM were stimulated with LPS in the presence or absence of COX inhibitors for the indicated periods. Both COX-1 and COX-2 inhibitors failed to inhibit mTREM-1 expression at 0.5 h after LPS stimulation, whereas mTREM-1 expression at 1 h was partially inhibited, and that at 2 and 4 h was significantly abolished by COX inhibitors (Fig. 4*C*). These findings indicated that the effect of $PGE_2$ on LPS-induced mTREM-1 expression was predominant at late time points (>2 h after stimulation) but not at early time points (0.5 and 1 h after stimulation).

After RPM were incubated with LPS in the presence or absence of COX inhibitors for various times, the expression of mTREM-1 protein was determined by Western blot analysis. Both inhibitors reduced LPS-induced TREM-1 expression at 4 and 8 h but not at 2 h after stimulation (Fig. 4*D*). Actin as the internal control was similarly detected in all samples. These findings indicated that LPS-induced expression of mTREM-1 on RPM was at least partly promoted by endogenous $PGE_2$.

### *$PGE_2$-induced TREM-1 expression is mediated by the EP4 receptor and cAMP*

It has been shown that the biological functions of $PGE_2$ are mediated by four specific receptors, which are coupled to G-protein and are referred to as EP1 to EP4 (20). To determine which EP receptors mediated $PGE_2$-induced mTREM-1 expression, RPM were incubated with four synthetic agonists specific for each of the EP receptors (each at a concentration of 1 μM), and then mTREM-1 expression was evaluated by quantitative real-time PCR. The EP4 agonist significantly up-regulated TREM-1 expression in RPM, whereas the EP1, EP2, and EP3 agonists failed to enhance TREM-1 expression (Fig. 5*A*).

Activation of the EP4 receptor enhances intracellular accumulation of cAMP via adenylate cyclase. Therefore, we examined the influence of 8-Br-cAMP (a stable cAMP analog) on mTREM-1 expression by RPM. Treatment of RPM with 8-Br-cAMP at a concentration of $5 \times 10^{-4}$ M for 1 h significantly enhanced expression of the *mTREM-1* gene by RPM (Fig. 5*B*). EP4 agonist and 8-Br-cAMP also induced TREM-1 mRNA expression in J774.1 and PBMC (data not shown). These finding clearly suggested that $PGE_2$-induced TREM-1 expression on RPM was related to EP4 receptor- and cAMP-mediated signaling.

### *Blocking of PKA, p38 MAPK, and PI3K inhibits $PGE_2$-induced mTREM-1 expression*

Intracellular cAMP is a major regulator of PKA (22) and cAMP also activates the PI3K-, p38 MAPK-, and ERK-signaling pathways (23–25). Therefore, we investigated the signaling pathways involved in $PGE_2$-induced expression of TREM-1 by using synthetic inhibitors of these kinases. A PKA inhibitor (H89), a p38 MAPK inhibitor (SB203580), and a PI3K inhibitor (LY294002) significantly suppressed $PGE_2$-induced TREM-1 expression, whereas a MAPKK inhibitor (PD98059) failed to influence TREM-1 expression (Fig. 6). Inhibitory effects of these inhibitors were observed in a dose- or time-dependent manner (data not shown). These results suggested that $PGE_2$-induced TREM-1 expression was mediated via the PKA, PI3K, and p38 MAPK pathways.

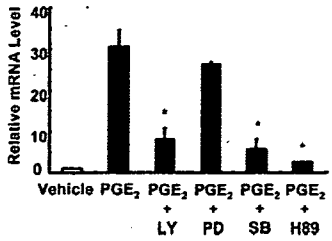


**FIGURE 6.** Inhibition of PKA, p38 MAPK, or PI3K suppresses $PGE_2$-induced mTREM-1 expression by RPM. RPM were pretreated with or without LY294002 (20 $\mu$M), PD98059 (30 $\mu$M), SB203580 (20 $\mu$M) H-89 (20 $\mu$M) for 30 min, and then were incubated with $PGE_2$ (1 $\mu$M) for 1 h. The mTREM-1 mRNA level was determined by quantitative real-time PCR. Data are expressed as the mean ± SD of triplicate determinations. *, $p < 0.01$ vs $PGE_2$-stimulated RPM by Student's unpaired $t$ test.

*Activation of TREM-1 significantly enhances cytokine production by $PGE_2$-treated PBMC*

An agonistic anti-TREM-1 mAb has been shown to stimulate the production of proinflammatory cytokines by monocytes (1, 7, 9). It was difficult to transfer $PGE_2$-treated RPM to Ab-coated wells, because the cells tightly adhere to the culture dishes. Therefore, PBMC were used to determine whether TREM-1 could enhance cytokine production by $PGE_2$-treated monocytes. Cells were incubated in the presence or absence of $PGE_2$ ($10^{-6}$ M) for 5 h, and then harvested for incubation in agonistic anti-TREM-1 mAb-coated wells for 24 h. Then the levels of TNF-$\alpha$ and IL-8 in the culture supernatant were determined by specific ELISAs. The agonistic anti-TREM-1 mAb caused a significant increase of TNF-$\alpha$ production by $PGE_2$-pretreated PBMC (Fig. 7*A*). Production of TNF-$\alpha$ by $PGE_2$-treated cells was 6-fold higher than that by untreated cells. The agonistic anti-TREM-1 mAb also increased IL-8 production by $PGE_2$-pretreated PBMC and the magnitude of this enhancement was 4.6-fold (Fig. 7*B*). These results indicated that

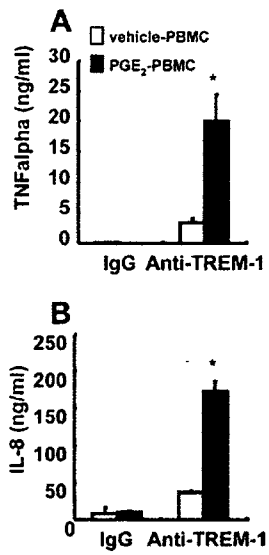


**FIGURE 7.** An agonistic anti-TREM-1 mAb enhances the production of proinflammatory cytokines by $PGE_2$-pretreated PBMC. PBMC were incubated with or without $PGE_2$ for 5 h, and then the cells were incubated in the presence or absence of the agonistic anti-TREM-1 mAb (5 $\mu$g/ml) or an isotype control Ab (5 $\mu$g/ml) for 24 h. Production of TNF-$\alpha$ (*A*) and IL-8 (*B*) was determined by specific ELISAs. Data are expressed as the mean ± SD of triplicate determinations. *, $p < 0.01$ vs vehicle-stimulated PBMC by Student's unpaired $t$ test.

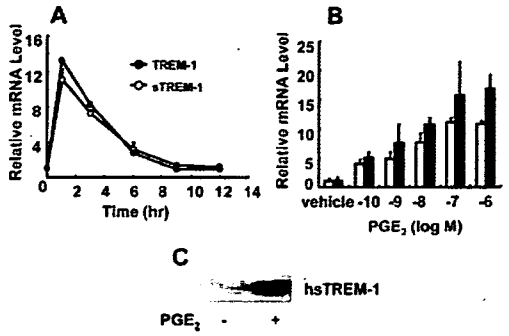


**FIGURE 8.** $PGE_2$ induces hTREM-1 and hsTREM-1 expression by PBMC in a time- and concentration-dependent manner. *A*, PBMC were incubated with $PGE_2$ (1 $\mu$M) for the indicated periods. Expression of the *hTREM-1* gene (○) and the *hsTREM-1* gene (●) was determined by real-time quantitative PCR. *B*, PBMC were cultured with or without various concentrations of $PGE_2$ for 1 h. Then the hTREM-1 (□) and hsTREM-1 (■) mRNA levels were determined by real-time quantitative PCR. *C*, PBMC were incubated with or without $PGE_2$ (1 $\mu$M) for 5 h and hsTREM-1 protein in the same volume of the supernatant (20$\mu$l) was determined by Western blot analysis. Data are expressed as the mean ± SD of triplicate determinations.

TREM-1 induced by $PGE_2$ was functional and enhanced the production of proinflammatory cytokines by PBMC.

*$PGE_2$ induces hTREM-1 and hsTREM-1 expression by PBMC*

It has been demonstrated that human monocytes are capable of expressing sTREM-1 as well as the cell surface form (3–5). Although sTREM-1 has also been identified in mice, the precise structure and function of soluble mTREM-1 are not yet known. Therefore, we investigated the expression of hTREM-1 and hsTREM-1 by $PGE_2$-treated PBMC to evaluate which type was predominantly expressed. After PBMC were incubated with $PGE_2$, *hTREM-1* and *hsTREM-1* gene expression were separately determined by quantitative real-time PCR.

Induction of both *hTREM-1* and *hsTRM-1* gene expression occurred quite rapidly and was seen as early as 1 h after stimulation, a subsequent declined until 9 h (Fig. 8*A*). To determine whether physiological concentrations of $PGE_2$ could induce the expression of hTREM-1 and hsTREM-1, PBMC were incubated with various concentrations of $PGE_2$ for 1 h and gene expression was determined. It was found that $PGE_2$ promoted both hTREM-1 and hsTREM-1 expression in a concentration-dependent manner, with maximal expression occurring at $10^{-6}$ or $10^{-7}$ M (Fig. 8*B*).

Western blot analysis using a specific anti-human TREM-1 mAb was performed to detect sTREM-1 protein. PBMC were incubated with or without $PGE_2$ for 5 h, and then the sTREM-1 protein level in the culture supernatant was determined by Western blotting. sTREM-1 was detected at very low levels when PBMC were incubated with the vehicle alone, whereas sTREM-1 expression was increased when PBMC were incubated with $PGE_2$ for 5 h (Fig. 8*C*). Taken together, these findings showed that $PGE_2$ up-regulated the expression of hTREM-1 as well as hsTREM-1 by monocytes.

## Discussion

The present study provided evidence that $PGE_2$ up-regulates mTREM-1 expression by RPM, as well as hTREM-1 and hsTREM-1 expression by human PBMC. LPS-induced TREM-1 expression is at least partly regulated by endogenous $PGE_2$, because COX inhibitors significantly reduced TREM-1 expression. $PGE_2$-induced TREM-1 expression was mediated by EP-4, cAMP, and various kinases such as PKA, PI3K, and p38 MAPK. $PGE_2$-induced TREM-1 was functional,

because agonistic anti-TREM-1 mAb promoted a significant increase in the production of TNF-$\alpha$ and IL-8.

It is known that TREM-1 is specifically up-regulated by microbial products such as LPS, lipoteichoic acid (LTA), or zymosan (1, 7, 9, 26). However, the present study provided the first demonstration that $PGE_2$ could induce TREM-1 expression by both RPM and PBMC. Induction of TREM-1 expression by $PGE_2$ was also observed in a human monocyte cell line (U937) and a murine macrophage cell line (J774.1) (data not shown), indicating that $PGE_2$ is an inducer of TREM-1 expression by both monocytes and macrophages. $PGE_2$ was a specific regulator of mTREM-1 expression, because specific ligands for the CRTH2 and TP receptors (which are expressed on macrophages) failed to induce mTREM-1 expression. Biological effect of endogenous $PGE_2$ on TREM-1 expression was predominant in the late phase of LPS-induced TREM-1 expression. This is based on the findings that COX inhibitors abrogated mTREM-1 expression after 2 h and also reduced mTREM-1 protein expression after 4–8 h following LPS stimulation.

In the present study, both COX-1 and COX-2 inhibitors suppressed $PGE_2$ synthesis and TREM-1 induction. It has been documented that LPS promoted $PGE_2$ production through the induction and activation of the COX-2, but not COX-1 (21, 27). However, Rouzer et al. (21) also reported that SC560 (COX-1 inhibitor) inhibits PG synthesis through inhibition of COX-2 as well as COX-1 in LPS-stimulated RPM. Because this cross-inhibition was not observed in other cells, it appeared to be specific in RPM. TNF-$\alpha$ is also an inducer of $PGE_2$ synthesis, but a previous study demonstrated that TNF-$\alpha$ had a limited effect on TREM-1 expression (7, 28). The reasons for this difference are not known, but it might be related to different mechanisms of action on monocytes and macrophages.

EP4, one of the receptors for $PGE_2$, increases intracellular cAMP levels via activation of adenylate cyclase and promotes activation of the PKA, PI3K, p38 MAPK, and MAPKK pathways (22–25). The present study demonstrated that a specific EP4 agonist and 8-Br-cAMP both enhanced *mTREM-1* gene expression, while inhibitors of PKA, p38 MAPK, and PI3K blocked the $PGE_2$-induced increase of mTREM-1 expression. These findings suggested that $PGE_2$-induced up-regulation of mTREM-1 expression was mediated by the binding of $PGE_2$ to EP4, which was followed by accumulation of cAMP and activation of various kinases, including PKA, p38 MAPK, and PI3K. This is consistent with the findings of previous studies demonstrating that $PGE_2$ potentially activate various kinases such as PKA, PI3K, and p38 MAPK independently (29, 30). COX inhibitors failed to completely suppress LPS-induced up-regulation of mTREM-1 expression by RPM, and these inhibitors abolished TREM-1 expression only in the late phase, but not early phase of LPS stimulation. These indicate that other pathways might also be involved in the induction of TREM-1 expression by LPS. Knapp et al. (28) recently demonstrated that a PI3K-dependent pathway played a central role, while MAPK also played a limited role, in LPS-induced up-regulation of TREM-1 expression by monocytes. Several signaling pathways might be involved in LPS-induced TREM-1 expression, and the endogenous $PGE_2$-mediated pathway seems to be one of the mechanisms of LPS-induced TREM-1 expression on monocytes and macrophages.

TLR and TREM-1 cooperate to induce an inflammatory response, because activation of TREM-1 causes a marked increment in the production of proinflammatory cytokines by macrophages when LPS is used as the costimulus (1, 8, 9). TREM-1 activates a downstream signaling pathway through DAP12, which involves tyrosine phosphorylation, activation of mitogen-activated protein kinases, and mobilization of $Ca^{2+}$. In contrast, TLRs directly recognize certain microbial products and components, such as LPS, LTA, and bacterial DNA. MyD88, IRAK, TRAF6, and IKK are essentially involved in the TLR-signaling pathway. These kinases can potentially induce the production of proinflammatory cytokines via the activation of NF-$\kappa$B (31). Natural ligands for TREM-1 remain to be identified. If specific ligands for TREM-1 are located at the foci of microbe-induced inflammation, interactions between TREM-1 and TLRs can synergistically induce inflammatory responses. In this case, cooperation between TLRs and TREM-1 could occur at several levels during the process of LPS-induced inflammation. The present study showed that an LPS-induced increase in the production of $PGE_2$ promoted TREM-1 expression, and activation of TREM-1 on $PGE_2$-treated PBMC enhanced the production of proinflammatory cytokines. Based on these findings, we hypothesized that $PGE_2$-induced up-regulation of TREM-1 expression may play an important role in enhancing the TLR-mediated response of macrophages to LPS stimulation.

Several line of evidence indicated that decoy receptors can modulate inflammatory responses by blocking the action by agonists (32, 33). sTREM-1 is a natural decoy receptor that could potentially inhibit TREM-1-mediated activation of cells through competition with natural ligand(s) for receptor binding. Synthetic sTREM-1 has been shown to inhibit LPS-induced cytokine production by monocytes in vitro (6). Furthermore, a recombinant sTREM-1 fusion protein and synthetic soluble TREM-1 have been shown to protect mice against lethal LPS challenge or bacterial sepsis by suppressing inflammatory cytokine production (6, 9). In contrast, it has been demonstrated that $PGE_2$ can suppress the production of various cytokines (such as TNF-$\alpha$, IL-8, MCP-1, IFN-$\gamma$-inducible protein-10, and MIP-1$\beta$) by LPS-stimulated macrophages through EP2- and/or EP4-mediated pathways (34, 35). $PGE_2$ also induces the production of IL-10, which can have an anti-inflammatory effect (36). Present study demonstrated that $PGE_2$ induced the release of sTREM-1 by PBMC. Therefore, $PGE_2$ might suppress inflammation not only by inhibiting the production of proinflammatory cytokines, but also by inducing expression of the decoy receptor sTREM-1 and increasing the production of IL-10. However, activation of TREM-1 on $PGE_2$-treated PBMC enhanced the production of proinflammatory cytokines, indicating that $PGE_2$ may exert bidirectional effects on monocytes and macrophages to modulate inflammation through altering the expression of TREM-1 and sTREM-1.

Blocking of PGs has been shown to increase LPS-induced cytokine production both in vitro and in vivo (36–39). This is consistent with the previous finding that $PGE_2$ and EP4 agonists attenuated LPS-induced cytokine production in mice (40). However, a number of studies have provided evidence that COX inhibitors can improve survival after the onset of endotoxic shock and COX-deficient mice are resistant to endotoxin-induced inflammation and death (17, 19, 41). Thus, the precise pathophysiological role of $PGE_2$ in microbe infection still remains undefined. Further investigations should be directed toward the in vivo effects of $PGE_2$-induced TREM-1 and sTREM-1 in sepsis models.

Increased expression of TREM-1 has been observed at sites of inflammation caused by microbial pathogens (9). However, we recently demonstrated that monosodium urate monohydrate (MSU) crystals induced mTREM-1 expression in monocytes and macrophages in vitro and in vivo (42), indicating that TREM-1 might be involved in the development of acute gouty arthritis. We also observed that MSU crystal-induced mTREM-1 expression is regulated, at least in part, by endogenous produced $PGE_2$ (our unpublished data). These findings suggest the possibility that $PGE_2$ might enhance TREM-1 expression in nonmicrobial inflammatory diseases including acute gouty arthritis. If a natural TREM-1 ligand is also induced in nonmicrobial inflammation, it could enhance inflammatory responses by activating $PGE_2$-induced

TREM-1. Furthermore, nonmicrobial products such as heat shock protein 60, which are induced in various inflammatory diseases, have been shown to stimulate TLRs (43). Thus, it is presumed that activation of $PGE_2$-induced TREM-1 and TLRs by specific ligands might cooperatively increase the inflammatory responses in patients with nonmicrobial inflammatory diseases.

The present study provided a first evidence that $PGE_2$ induces the expression of both TREM-1 and sTREM-1 by macrophages. This finding sheds new light on the role of $PGE_2$ as a regulator of the inflammatory response to microbial infection. Further investigations should be directed toward the assessment of pathophysiological roles of TREM-1 and sTREM-1 in various inflammatory diseases. Such studies may help to elucidate the precise role of $PGE_2$-induced TREM-1 expression in inflammation and could possibly provide evidence leading to new strategies for the treatment of inflammatory diseases.

## Acknowledgments

We thank Rie Hasegawa and Mitsuko Mizuno for their technical support.

## Disclosures

The authors have no financial conflict of interest.

## References

1. Bouchon, A., J. Dietrich, and M. Colonna. 2000. Inflammatory responses can be triggered by TREM-1, a novel receptor expressed on neutrophils and monocytes. *J. Immunol.* 164: 4991–4995.
2. Colonna, M., and F. Facchetti. 2003. TREM-1 (triggering receptor expressed on myeloid cells): a new player in acute inflammatory responses. *J. Infect. Dis.* 187: S397–S401.
3. Allaouchiche, B., and E. Boselli. 2004. Soluble TREM-1 and the diagnosis of pneumonia. *N. Engl. J. Med.* 350: 1904–1905.
4. Gibot, S., M. N. Kolopp-Sarda, M. C. Bene, A. Cravoisy, B. Levy, G. C. Faure, and P. E. Bollaert. 2004. Plasma level of a triggering receptor expressed on myeloid cells-1: its diagnostic accuracy in patients with suspected sepsis. *Ann. Intern. Med.* 141: 9–15.
5. Gingras, M. C., H. Lapillonne, and J. F. Margolin. 2002. TREM-1, MDL-1, and DAP12 expression is associated with a mature stage of myeloid development. *Mol. Immunol.* 38: 817–824.
6. Gibot, S., M. N. Kolopp-Sarda, M. C. Bene, P. E. Bollaert, A. Lozniewski, F. Mory, B. Levy, and G. C. Faure. 2004. A soluble form of the triggering receptor expressed on myeloid cells-1 modulates the inflammatory response in murine sepsis. *J. Exp. Med.* 200: 1419–1426.
7. Bleharski, J. R., V. Kiessler, C. Buonsanti, P. A. Sieling, S. Stenger, M. Colonna, and R. L. Modlin. 2003. A role for triggering receptor expressed on myeloid cells-1 in host defense during the early-induced and adaptive phases of the immune response. *J. Immunol.* 170: 3812–3818.
8. Colonna, M. 2003. TREMs in the immune system and beyond. *Nat. Rev. Immunol.* 3: 445–453.
9. Bouchon, A., F. Facchetti, M. A. Weigand, and M. Colonna. 2001. TREM-1 amplifies inflammation and is a crucial mediator of septic shock. *Nature* 410: 1103–1107.
10. Marnett, L. J., S. W. Rowlinson, D. C. Goodwin, A. S. Kalgutkar, and C. A. Lanzo. 1999. Arachidonic acid oxygenation by COX-1 and COX-2: mechanisms of catalysis and inhibition. *J. Biol. Chem.* 274: 22903–22906.
11. Bertelsen, L. S., G. Paesold, L. Eckmann, and K. E. Barrett. 2003. *Salmonella* infection induces a hypersecretory phenotype in human intestinal xenografts by inducing cyclooxygenase 2. *Infect. Immun.* 71: 2102–2109.
12. Lopez-Urrutia, L., A. Alonso, Y. Bayon, M. L. Nieto, A. Orduna, and M. Sanchez Crespo. 2001. *Brucella* lipopolysaccharides induce cyclooxygenase-2 expression in monocytic cells. *Biochem. Biophys. Res. Commun.* 289: 372–375.
13. Anderson, F. L., W. Jubiz, T. J. Tsagaris, and H. Kuida. 1975. Endotoxin-induced prostaglandin E and F release in dogs. *Am. J. Physiol.* 228: 410–414.
14. Kessler, E., R. C. Hughes, E. N. Bennett, and S. M. Nadela. 1973. Evidence for the presence of prostaglandin-like material in the plasma of dogs with endotoxin shock. *J. Lab. Clin. Med.* 81: 85–94.
15. Strassmann, G., V. Patil-Koota, F. Finkelman, M. Fong, and T. Kambayashi. 1994. Evidence for the involvement of interleukin 10 in the differential deactivation of murine peritoneal macrophages by prostaglandin $E_2$. *J. Exp. Med.* 180: 2365–2370.
16. Portanova, J. P., Y. Zhang, G. D. Anderson, S. D. Hauser, J. L. Masferrer, K. Seibert, S. A. Gregory, and P. C. Isakson. 1996. Selective neutralization of prostaglandin $E_2$ blocks inflammation, hyperalgesia, and interleukin 6 production in vivo. *J. Exp. Med.* 184: 883–891.
17. Wise, W. C., J. A. Cook, T. Eller, and P. V. Halushka. 1980. Ibuprofen improves survival from endotoxic shock in the rat. *J. Pharmacol. Exp. Ther.* 215: 160–164.
18. Shoup, M., L. K. He, H. Liu, R. Shankar, and R. Gamelli. 1998. Cyclooxygenase-2 inhibitor NS-398 improves survival and restores leukocyte counts in burn infection. *J. Trauma* 45: 215–220.
19. Jacobs, E. R., M. E. Soulsby, R. C. Bone, F. J. Wilson, Jr., and F. C. Hiller. 1982. Ibuprofen in canine endotoxin shock. *J. Clin. Invest.* 70: 536–541.
20. Tilley, S. L., T. M. Coffman, and B. H. Koller. 2001. Mixed messages: modulation of inflammation and immune responses by prostaglandins and thromboxanes. *J. Clin. Invest.* 108: 15–23.
21. Rouzer, C. A., P. J. Kingsley, H. Wang, H. Zhang, J. D. Morrow, S. K. Dey, and L. J. Marnett. 2004. Cyclooxygenase-1-dependent prostaglandin synthesis modulates tumor necrosis factor-$\alpha$ secretion in lipopolysaccharide-challenged murine resident peritoneal macrophages. *J. Biol. Chem.* 279: 34256–34268.
22. Taylor, S. S., J. Yang, J. Wu, N. M. Haste, E. Radzio-Andzelm, and G. Anand. 2004. PKA: a portrait of protein kinase dynamics. *Biochim. Biophys. Acta* 1697: 259–269.
23. Cass, L. A., S. A. Summers, G. V. Prendergast, J. M. Backer, M. J. Birnbaum, and J. L. Meinkoth. 1999. Protein kinase A-dependent and -independent signaling pathways contribute to cyclic AMP-stimulated proliferation. *Mol. Cell Biol.* 19: 5882–5891.
24. Fiebich, B. L., S. Schleicher, O. Spleiss, M. Czygan, and M. Hull. 2001. Mechanisms of prostaglandin $E_2$-induced interleukin-6 release in astrocytes: possible involvement of EP4-like receptors, p38 mitogen-activated protein kinase and protein kinase C. *J. Neurochem.* 79: 950–958.
25. Busca, R., P. Abbe, F. Mantoux, E. Aberdam, C. Peyssonnaux, A. Eychene, J. P. Ortonne, and R. Ballotti. 2000. Ras mediates the cAMP-dependent activation of extracellular signal-regulated kinases (ERKs) in melanocytes. *EMBO J.* 19: 2900–2910.
26. Nochi, H., N. Aoki, K. Oikawa, M. Yanai, Y. Takiyama, Y. Atsuta, H. Kobayashi, K. Sato, M. Tateno, T. Matsuno, et al. 2003. Modulation of hepatic granulomatous responses by transgene expression of DAP12 or TREM-1-Ig molecules. *Am. J. Pathol.* 162: 1191–1201.
27. Gray, T., P. Nettesheim, C. Loftin, J. S. Koo, J. Bonner, S. Peddada, and R. Langenbach. 2004. Interleukin-1$\beta$-induced mucin production in human airway epithelium is mediated by cyclooxygenase-2, prostaglandin $E_2$ receptors, and cyclic AMP-protein kinase A signaling. *Mol. Pharmacol.* 66: 337–346.
28. Knapp, S., S. Gibot, A. de Vos, H. H. Versteeg, M. Colonna, and T. van der Poll. 2004. Expression patterns of surface and soluble triggering receptor expressed on myeloid cells-1 in human endotoxemia. *J. Immunol.* 173: 7131–7134.
29. Fujino, H., S. Salvi, and J. W. Regan. 2005. Differential regulation of phosphorylation of the cAMP response element-binding protein after activation of EP2 and EP4 prostanoid receptors by prostaglandin $E_2$. *Mol. Pharmacol.* 68: 251–259.
30. Caristi, S., G. Piraino, M. Cucinotta, A. Valenti, S. Loddo, and D. Teti. 2005. Prostaglandin $E_2$ induces interleukin-8 gene transcription by activating C/EBP homologous protein in human T lymphocytes. *J. Biol. Chem.* 280: 14433–14442.
31. Takeda, K., and S. Akira. 2005. Toll-like receptors in innate immunity. *Int. Immunol.* 17: 1–14.
32. Arend, W. P. 1991. Interleukin 1 receptor antagonist: a new member of the interleukin 1 family. *J. Clin. Invest.* 88: 1445–1451.
33. Abramson, S. B., and A. Amin. 2002. Blocking the effects of IL-1 in rheumatoid arthritis protects bone and cartilage. *Rheumatology* 41: 972–980.
34. Takayama, K., G. Garcia-Cardena, G. K. Sukhova, J. Comander, M. A. Gimbrone, Jr, and P. Libby. 2002. Prostaglandin $E_2$ suppresses chemokine production in human macrophages through the EP4 receptor. *J. Biol. Chem.* 277: 44147–44154.
35. Treffkorn, L., R. Scheibe, T. Maruyama, and P. Dieter. 2004. $PGE_2$ exerts its effect on the LPS-induced release of TNF-$\alpha$, ET-1, IL-1$\alpha$, IL-6 and IL-10 via the EP2 and EP4 receptor in rat liver macrophages. *Prostaglandins Other Lipid Mediat.* 74: 113–123.
36. Dong, Y. L., D. N. Herndon, T. Z. Yan, and J. P. Waymack. 1993. Blockade of prostaglandin products augments macrophage and neutrophil tumor necrosis factor synthesis in burn injury. *J. Surg. Res.* 54: 480–485.
37. Ertel, W., M. H. Morrison, P. Wang, Z. F. Ba, A. Ayala, and I. H. Chaudry. 1991. The complex pattern of cytokines in sepsis: association between prostaglandins, cachectin, and interleukins. *Ann. Surg.* 214: 141–148.
38. Sacco, S., D. Agnello, M. Sottocorno, G. Lozza, A. Monopoli, P. Villa, and P. Ghezzi. 1998. Nonsteroidal anti-inflammatory drugs increase tumor necrosis factor production in the periphery but not in the central nervous system in mice and rats. *J. Neurochem.* 71: 2063–2070.
39. Sironi, M., M. Gadina, M. Kankova, F. Riganti, A. Mantovani, M. Zandalasini, and P. Ghezzi. 1992. Differential sensitivity of in vivo TNF and IL-6 production to modulation by anti-inflammatory drugs in mice. *Int. J. Immunopharmacol.* 14: 1045–1050.
40. Sakamoto, A., J. Matsumura, S. Mii, Y. Gotoh, and R. Ogawa. 2004. A prostaglandin $E_2$ receptor subtype EP4 agonist attenuates cardiovascular depression in endotoxin shock by inhibiting inflammatory cytokines and nitric oxide production. *Shock* 22: 76–81.
41. Ejima, K., M. D. Layne, I. M. Carvajal, P. A. Kritek, R. M. Baron, Y. H. Chen, J. Vom Saal, B. D. Levy, S. F. Yet, and M. A. Perrella. 2003. Cyclooxygenase-2-deficient mice are resistant to endotoxin-induced inflammation and death. *FASEB J.* 17: 1325–1327.
42. Murakami, Y., T. Akahoshi, I. Hayashi, H. Endo, S. Kawai, M. Inoue, H. Kondo, and H. Kitasato. 2006. Induction of triggering receptor expressed on myeloid cells 1 in murine resident peritoneal macrophages by monosodium urate monohydrate crystals. *Arthritis Rheum.* 54: 455–462.
43. Sharif, M., J. G. Worrall, B. Singh, R. S. Gupta, P. M. Lydyard, C. Lambert, J. McCulloch, and G. A. Rook. 1992. The development of monoclonal antibodies to the human mitochondrial 60-kd heat-shock protein, and their use in studying the expression of the protein in rheumatoid arthritis. *Arthritis Rheum.* 35: 1427–1433.

ARTHRITIS & RHEUMATISM
Vol. 56, No. 4, April 2007, pp 1304–1314
DOI 10.1002/art.22521


# A New Murine Model to Define the Critical Pathologic and Therapeutic Mediators of Polymyositis

Takahiko Sugihara,[1] Chiyoko Sekine,[2] Takashi Nakae,[3] Kuniko Kohyama,[4] Masayoshi Harigai,[5] Yoichiro Iwakura,[6] Yoh Matsumoto,[4] Nobuyuki Miyasaka,[5] and Hitoshi Kohsaka[1]

*Objective.* **To establish a new murine model of polymyositis (PM) for the understanding of its pathologic mechanisms and the development of new treatment strategies.**

*Methods.* **C protein–induced myositis (CIM) was induced by a single immunization of recombinant human skeletal C protein in C57BL/6 mice, as well as in CD4-depleted, CD8-depleted, and mutant mice as controls. Some mice were treated with high-dose intravenous immunoglobulin (IVIG) after disease induction. Muscle tissues were examined histologically.**

*Results.* **In mice with CIM, inflammation was confined to the skeletal muscles. Histologic examination revealed a common pathologic feature of CIM and PM, involving abundant infiltration of CD8 and perforin-expressing cells in the endomysial site of the injured muscle. Suppression of myositis was achieved by depletion of both CD4 and CD8 T cells. Despite the development of serum anti–C protein antibodies in wild-type mice, severe myositis was induced in mice deficient in B cells. Induction of myositis was suppressed in interleukin-1$\alpha/\beta$ (IL-1$\alpha/\beta$)–null mutant mice, but not in tumor necrosis factor $\alpha$ (TNF$\alpha$)–null mutant mice. Use of IVIG, a treatment with proven efficacy in PM, suppressed CIM in the subgroup of treated mice.**

*Conclusion.* **CIM mimics PM pathologically and clinically. Infiltration of CD8 T cells is the most likely mechanism of muscle injury, and IL-1, but not B cells or TNF$\alpha$, is crucial in the development of CIM. IVIG has therapeutic effects in CIM, suggesting that the effects of IVIG are not mediated by suppression of antibody-mediated tissue injury. This murine model provides a useful tool for understanding the pathologic mechanisms of PM and for developing new treatment strategies.**

Polymyositis (PM) is a chronic autoimmune inflammatory myopathy affecting striated muscles (1). Damage of muscles results in varying degrees of muscle weakness. Dysphagia with choking episodes and respiratory muscle weakness can occur in acute cases of PM. Currently, the pathogenesis of PM is unknown, and patients are therefore treated with nonspecific immunosuppressants. High-dose corticosteroids are the first-line treatment but are not effective in all patients. Improvement of disease often depends on the dosage of corticosteroids, making a dosage reduction difficult and thus, in many cases, necessitating administration of methotrexate or other immunosuppressants as adjunctive treatment. Because these medications can elicit a wide variety of adverse drug reactions, new therapies to address the specific pathologic features of PM are needed.

In affected muscles of patients with PM, infiltration of mononuclear cells leads to muscle fiber necrosis. These cells are found in the endomysial site, where non-necrotic muscle fibers are damaged, and also in the perimysial and perivascular sites of the muscles. Immunohistochemical studies have disclosed that CD8 T cells are most abundant in the endomysial site and invade

Supported by grants-in-aid from the Japanese Ministry of Education, Culture, Sports, Science, and Technology and from the Japanese Ministry of Health, Labor and Welfare.

[1]Takahiko Sugihara, MD, Hitoshi Kohsaka, MD, PhD: Tokyo Medical and Dental University, Tokyo, Japan, and Research Center for Allergy and Immunology, RIKEN, Yokohama, Japan; [2]Chiyoko Sekine, PhD: Research Center for Allergy and Immunology, RIKEN, Yokohama, Japan; [3]Takashi Nakae: Benesis Corporation, Osaka, Japan; [4]Kuniko Kohyama, MS, Yoh Matsumoto, MD, PhD: Tokyo Metropolitan Institute for Neuroscience, Tokyo, Japan; [5]Masayoshi Harigai, MD, PhD, Nobuyuki Miyasaka, MD, PhD: Tokyo Medical and Dental University, Tokyo, Japan; [6]Yoichiro Iwakura, DSc: University of Tokyo, Tokyo, Japan.

Address correspondence and reprint requests to Hitoshi Kohsaka, MD, PhD, Department of Medicine and Rheumatology, Graduate School, Tokyo Medical and Dental University, 1-5-45 Yushima, Bunkyo-ku, Tokyo 113-8519, Japan. E-mail: kohsaka.rheu@tmd.ac.jp.

Submitted for publication March 31, 2006; accepted in revised form January 16, 2007.

non-necrotic muscle fibers (2,3). These CD8 T cells express cytotoxic effector molecules, known as perforins, that are oriented toward target muscle fibers (4). Surface expression of class I major histocompatibility complex (MHC) molecules on muscle fibers is up-regulated (5). In a study of T cells from patients with PM compared with normal donors, CD8 T cell clones expanded more frequently in the peripheral blood of patients with PM (6,7). Moreover, some of these clones could be found in muscle biopsy samples from the same patients (6,7). All of these observations support the view that PM is driven by cytotoxic CD8 T cells.

In rheumatoid arthritis (RA), another autoimmune disease, biologic agents that block tumor necrosis factor $\alpha$ (TNF$\alpha$) have been introduced into clinical use. TNF$\alpha$ blockade has an enormous effect in modulating the clinical course of RA (8). Animal models of arthritis serve to help identify therapeutic targets and to test the effect of these therapeutic reagents (9–11). In contrast, in PM, the lack of appropriate animal models has hampered basic research studies and delayed the development of new treatments.

Experimental autoimmune myositis (EAM), established previously as an animal model of PM, is inducible specifically in SJL/J mice by repeated administration of muscle homogenate or partially purified myosin (12,13). This model is a complex representation of disease, because SJL/J mice have a dysferlin gene mutation that causes spontaneous muscle necrosis and secondary muscle inflammation (14). Immunohistochemical studies have shown that infiltrating T cells in the muscle are dominated by CD4 T cells, suggesting that the EAM disease model is mediated by CD4 T cells (15).

We established a new murine model that can be induced with a single injection of a recombinant skeletal muscle fast-type C protein. This myosin-binding protein is in the cross-bridge–bearing zone of A bands of myofibrils (16,17). Biochemical purification studies showed that C protein appears to be the main immunopathogenic component of the crude skeletal-muscle myosin preparation used for the induction of experimental myositis in Lewis rats (18,19). In this study, we used recombinant protein fragments to confirm the immunogenicity of the C protein. This myositis, designated as C protein–induced myositis (CIM), can be induced in C57BL/6 (B6) mice and in other strains of mice. Its histologic and immunohistochemical features mimic those of PM. Functional studies have indicated that cytotoxic CD8 T cells are primarily responsible for the pathologic mechanisms of this disease.

Susceptibility to CIM in B6 mice has facilitated studies of the immunologic components required to induce myositis. In the present study, we were able to show that the effects of immunoglobulins are not necessary for the development of CIM, despite the presence of B cells in the affected muscles and anti–C protein antibodies in the sera. Although both interleukin-1 (IL-1)–positive and TNF$\alpha$-positive cells infiltrated the muscles of affected mice, only IL-1, not TNF$\alpha$, was crucial in the development of CIM. Interestingly, CIM was suppressed by infusion of intravenous immunoglobulins (IVIGs), which has been used as a last resort for treatment of patients with PM who do not respond to or tolerate immunosuppressive reagents. Thus, we show that our new model is useful in investigating the pathologic mechanisms of autoimmune myositis and in developing new treatment strategies for this disease.

## MATERIALS AND METHODS

**Mice.** B6, SJL/J, BALB/c, DBA/1, and C3H/He mice were purchased from Charles River (Yokohama, Japan). NZB and MRL/Mp+/+ mice were purchased from SLC (Shizuoka, Japan). Mutant B6 mice rendered double-null for IL-1$\alpha/\beta$ were established previously (20), while Ig$\mu$-null mutant B6 mice (21) and TNF$\alpha$-null mutant mice (22) were kindly provided by Drs. Karasuyama (Tokyo Medical and Dental University) and Sekikawa (formerly at the National Institute of Agrobiological Science), respectively. All experiments were done under specific pathogen–free conditions in accordance with the ethics and safety guidelines for animal experiments of Tokyo Medical and Dental University and RIKEN.

**Recombinant human skeletal C protein.** Four complementary DNA (cDNA) fragments encoding overlapping cDNA fragments 1, 2, 3, and 4 of human fast-type skeletal muscle C protein were amplified from human skeletal muscle cDNA using polymerase chain reaction. Primers used were 5′-GAGAGGTACCATGCCTGAGGCAAAACCAGCG-3′ and 5′-GAGAGTCGACTCAGAACCACTTGAGGGTCAGGTC-3′ for fragment 1, 5′-GAGAGGATCCGACCTGACCCTCAAGTGGTTC-3′ and 5′-GAGAAAGCTTTCACAGCCAGGTAGCGACGGGAGG-3′ for fragment 2, 5′-AGAGGATCCCCTCCCGTCGCTACCTGGCTG-3′ and 5′-GAGAAAGCTTTCACCGGGGCTTTCCCTGGAAGGG-3′ for fragment 3, and 5′-AGAGGATCCCCCTTCAGGGAAAGCCCCGG-3′ and 5′-GAGAAAGCTTTCACTGCGGCACTCGGACCTC-3′ for fragment 4 (Qiagen, Hilden, Germany) (underlining indicates the restriction enzyme recognition sites for subcloning into the pQE30 expression vector). These primers were introduced into the TOP10F′ bacterial host (Invitrogen, Carlsbad, CA) and were used to prepare recombinant C protein fragments according to the manufacturer's protocol. Soluble recombinant C proteins were dialyzed against 0.5*M* arginine, 2 m*M* reduced glutathione, 0.2 m*M* oxydized glutathione in phosphate buffered saline (PBS), pH 7.4 (fragments 1 and 2) or 25 m*M* glycine HCl, pH 3.0

(fragments 3 and 4). Endotoxin was removed using Detoxi-Gel Endotoxin Removal Gel (Pierce, Rockford, IL).

**Induction of CIM.** Female mice, ages 8–10 weeks, were immunized intradermally with 200 μg of the C protein fragments emulsified in Freund's complete adjuvant (CFA) containing 100 μg of heat-killed *Mycobacterium butyricum* (Difco, Detroit, MI). The immunogens were injected at multiple sites of the back and foot pads, and 2 μg of pertussis toxin (PT) (Seikagaku Kogyo, Tokyo, Japan) in PBS was injected intraperitoneally at the same time. Hematoxylin and eosin–stained 10-μm sections of the proximal muscles (hamstrings and quadriceps) were examined histologically for the presence of mononuclear cell infiltration and necrosis of muscle fibers. The histologic severity of inflammation in each muscle block was graded as follows (18,19): grade 1 = involvement of a single muscle fiber or <5 muscle fibers; grade 2 = a lesion involving 5–30 muscle fibers; grade 3 = a lesion involving a muscle fasciculus; and grade 4 = diffuse, extensive lesions. When multiple lesions with the same grade were found in a single muscle block, 0.5 point was added to the grade.

**Immunohistochemical analysis.** Cryostat-frozen sections (6 μm) fixed in cold acetone were stained with anti-CD8a (53-6.7; BD Biosciences PharMingen, San Diego, CA), anti-CD4 (H129.19; BD Biosciences PharMingen), anti-B220 (RA3-6B2; BD Biosciences PharMingen), anti-CD11b (M1/70; BD Biosciences PharMingen), anti-CD68 (FA-11; Serotec, Oxford, UK), anti–IL-1α (40508; Genzyme/Techne, Minneapolis, MN), or anti-TNFα (MP6-XT22; BioLegend, San Diego, CA) monoclonal antibodies (mAb). To stain perforin molecules, air-dried sections were treated with 0.5% periodic acid solution and then stained with antiperforin mAb (CB5.4; Alexis Biochemicals, San Diego, CA). Nonspecific staining was blocked with 4% Blockace (Dainippon, Osaka, Japan).

Bound antibodies were visualized with peroxidase-labeled anti-rat IgG antibodies and associated substrates (Histofine Simple Stain Max PO; Nichirei, Tokyo, Japan). The sections were also stained with biotinylated mouse anti-mouse H-2K$^b$ mAb (AF6-88.5; BD Biosciences PharMingen) and with biotinylated mouse anti-mouse I-A$^b$ mAb (AF6-120.1; BD Biosciences PharMingen). They were then incubated with peroxidase-conjugated streptavidin and its substrates (Chemicon, Temecula, CA). For double immunofluorescence staining, the sections were preincubated with 5% heat-inactivated rat serum and 1% bovine serum albumin, and were stained with Alexa Fluor 647–conjugated anti-CD8a mAb (53-6.7; BD Biosciences PharMingen) and fluorescein isothiocyanate (FITC)–conjugated anti-CD4 mAb (RM4-5; BD Biosciences PharMingen).

The bound antibodies were visualized using SP2AOBS confocal laser microscopy (Leica, Heidelberg, Germany). Spleens or popliteal lymph nodes were stained as positive controls. Isotype controls were used as negative control. The stained sections were evaluated by 2 independent observers, who reported results that were comparable.

**Quantification of mononuclear cell subsets.** The method used to quantify stained cells in the immunohistochemical analysis was based on a previously published method (2). Briefly, 5 inflammatory mononuclear cell foci in the serial sections from 4 mice with CIM were studied. At least 1 focus from each mouse was evaluated. Stained mononuclear cells infiltrating into the endomysial, perimysial, and perivascular sites of the foci were enumerated separately. The frequency of each subset was calculated in relation to the sum of all subsets. The CD4:CD8 ratios were calculated on the basis of these calculations. The CD4:CD8 ratios in double immunofluorescence staining were calculated in the same manner as in the immunohistochemical analyses. CD68-positive and CD11b-positive cells in the serial sections were also enumerated in the same manner, and the frequencies of CD68-positive cells were calculated in relation to the number of CD11b-positive cells.

**Rotarod test.** Muscle function was evaluated with a MK-630 rotarod device (Muromachi Kikai, Tokyo, Japan) as described previously (23). The rotarod test was performed on each mouse by measuring the running time until the mouse fell off the rod while the rod was turning at 20 revolutions per minute for 200 seconds. The running ability of each mouse was scored in 5 categories of running time: score 1 = 0–49 seconds, score 2 = 50–99 seconds, score 3 = 100–149 seconds, score 4 = 150–200 seconds, score 5 = >200 seconds. Mice were initially trained to accommodate them to the task, and then tested 2 days thereafter.

**In vivo depletion of CD8 or CD4 T cells.** For the depletion of CD8 or CD4 T cells in B6 mice, the mice were injected intraperitoneally with 1 mg of purified anti-CD8 (53.67.2) mAb (24), anti-CD4 (GK1.5) mAb (24), or purified rat IgG (Sigma-Aldrich, St. Louis, MO) as a control, for 3 consecutive days. This treatment started 10 days before the immunization. Injection of 500 μg of the same mAb was repeated every other day for 14 days. Splenocytes and lymph node cells from the treated mice were stained with phycoerythrin (PE)–conjugated anti-CD8 mAb (53.67; BD Biosciences PharMingen) or PE-conjugated anti-CD4 mAb (H129.19; BD Biosciences PharMingen), together with FITC-conjugated anti-CD3 mAb (145-2C11; BD Biosciences PharMingen). The cells were then analyzed with FACSCalibur (Becton Dickinson, San Jose, CA).

**IVIG treatment.** A subgroup of the mice were treated with IVIG. Human gamma immunoglobulins (Venoglobulin-IH; Benesis, Osaka, Japan) (400 mg/kg/day) were injected intravenously into the tail vein for 5 consecutive days, beginning 3 days after immunization.

**Statistical analysis.** Histologic scores were compared with the Mann-Whitney U test. *P* values less than or equal to 0.05 were considered significant.

## RESULTS

**Histologic features of CIM in immunized mice.** Recombinant human fast-type skeletal C protein fragments were prepared using a prokaryotic expression system. Because of the size of the C protein, 4 overlapping protein fragments were generated: fragment 1 (amino acids 1–290), fragment 2 (amino acids 284–580), fragment 3 (amino acids 567–877), and fragment 4 (amino acids 864–1142). B6 mice were immunized at multiple sites of the back and foot pads with each fragment emulsified in CFA. PT was also injected intraperitoneally. To compare the immunogenicity of the 4 fragments, 5 mice per group were immunized with each

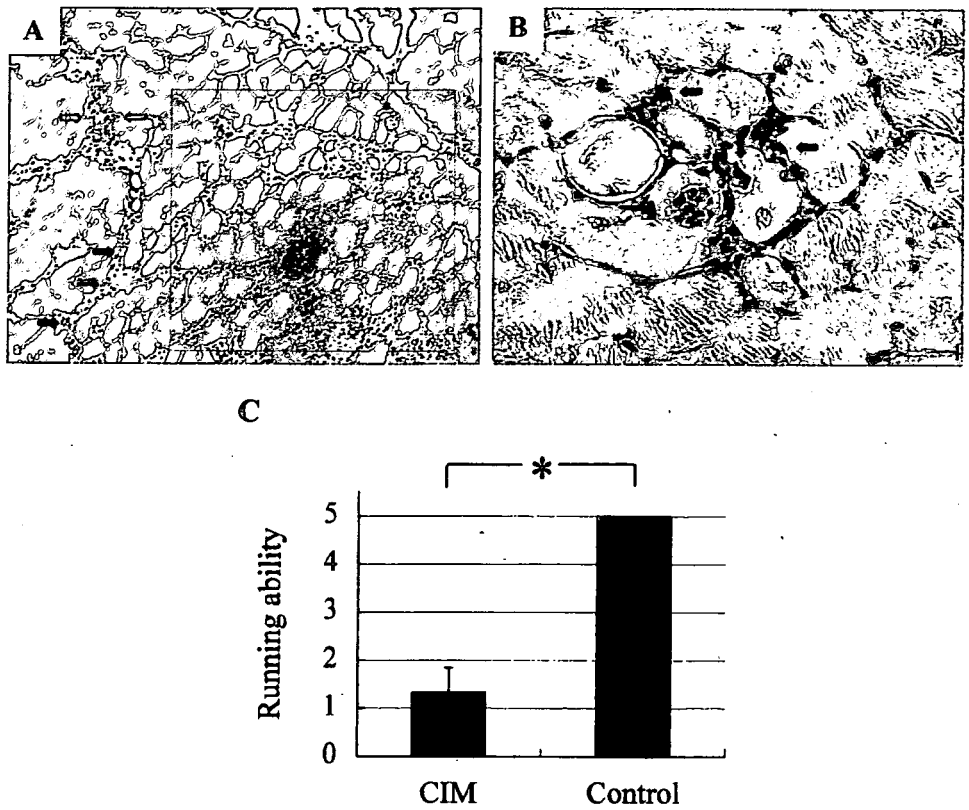


**Figure 1.** Muscle inflammation in C protein–induced myositis (CIM). C57BL/6 mice were immunized once with recombinant human skeletal C protein fragment 2 to induce CIM. **A** and **B,** Mononuclear cell infiltration was found predominantly in the endomysial site (boxed area) but also in the perimysial site (**solid arrows**) and perivascular site (**open arrows**) (**A**). Many cells invaded non-necrotic muscle fibers (**arrows**), while necrotic fibers were also present (**B**). Bar in **A** = 100 μm; bar in **B** = 25 μm. **C,** Muscle function was evaluated with a rotarod test 21 days after immunization. Six mice with CIM and 5 control mice treated with adjuvant alone were examined. Running ability was scored as described in Materials and Methods. Values are the mean and SD score. * = $P < 0.01$.

fragment, and myositis was studied histologically 21 days after the immunizaton.

None of the mice treated with adjuvant alone or immunized without PT developed myositis. We found that a single immunization of fragments 2 or 4 induced myositis consistently, and the mean ± SD histologic scores were 2.8 ± 0.2 and 1.0 ± 0.3, respectively. Fragments 1 and 3 induced milder myositis at a lower incidence, and the mean ± SD histologic scores were 0.2 ± 0.3 and 0.1 ± 0.2, respectively. Because fragment 2 induced the most severe myositis, it was used as an immunogen in subsequent experiments.

Histologic analysis of the muscles affected by CIM showed that mononuclear cells infiltrated predominantly the endomysial site, but also the perimysial and perivascular sites of the muscle tissue (Figure 1A). Many mononuclear cells invaded non-necrotic muscle fibers (Figure 1B). No abnormality in cardiac muscle and other tissues, including lung and joint tissues, was observed. Muscle function was assessed clinically with a rotarod device on day 21. Consistent with the histologic findings in the muscle tissue, mice with CIM ran for a shorter time than did control mice, indicating a reduction in motor function (Figure 1C).

Inflammation is acute and regresses spontaneously in most animal models of autoimmune diseases. To study the course of CIM in mice, muscle sections from 4 or 5 mice were examined at various time points after the immunization. A small number of mononuclear cells appeared in 50% of the muscle samples on day 7

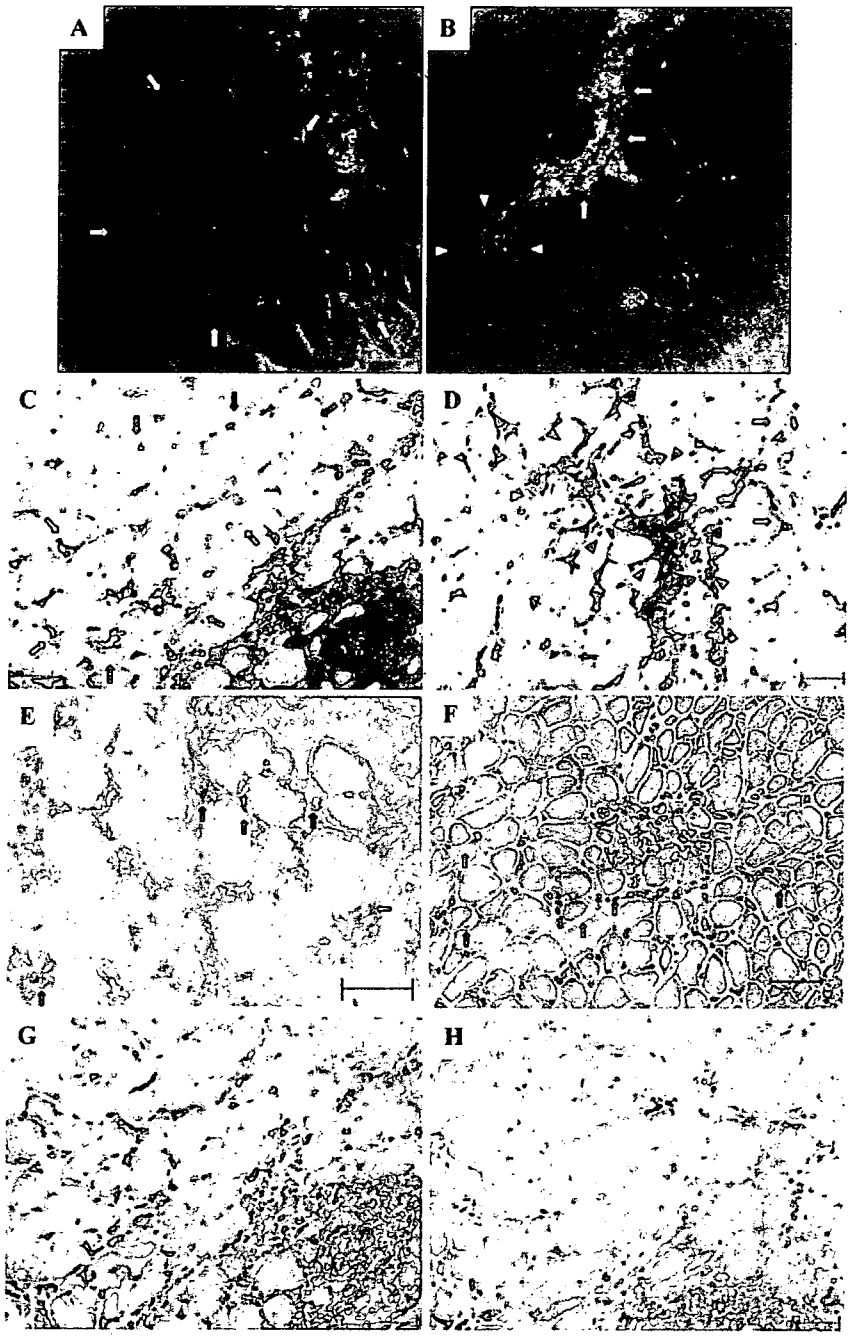


**Figure 2.** Immunohistochemical findings in muscles of mice with C protein–induced myositis. **A** and **B**, Expression of CD4 (green, fluorescein isothiocyanate) and CD8 (red, Alexa Fluor 647) was examined. Infiltrating cells in the endomysial site (**arrows**) (**A**) and in the perimysial site (**arrows**) and perivascular site (**arrowheads**) (**B**) were individually enumerated for calculating CD4:CD8 ratios. **C–H**, Expression of CD11b (**C** and **D**), perforin (**E**), class I major histocompatibility complex (**F**), interleukin-1$\alpha$ (IL-1$\alpha$) (**G**), and tumor necrosis factor $\alpha$ (TNF$\alpha$) (**H**) was examined with immunoperoxidase staining. CD11b-positive cells diffusely infiltrated the endomysial site (**arrows**) (**C**) and both the perimysial (**arrows**) and perivascular sites (**arrowheads**) (**D**). Perforin-positive cells infiltrated around non-necrotic muscle fibers at the endomysial sites (**arrows**) (**E**). Muscle fibers reacted to anti-H2K$^b$ monoclónal antibodies (**arrows**) (**F**). IL-1$\alpha$ and TNF$\alpha$ were expressed on infiltrating mononuclear cells in muscles (**G** and **H**). Bars = 50 $\mu$m.